Functionalized Starch Nanoparticles for Pulp-Based Active Packaging

by

Stephen Wei

A thesis
presented to the University of Waterloo
in the fulfillment of the
thesis requirement for the degree of
Master of Applied Science
In
Chemical Engineering (Nanotechnology)

Waterloo, Ontario, Canada, 2018

Author’s Declaration

I hereby declare that I am the sole author of this thesis. This is a true copy of the thesis, including any required final revisions, as accepted by my examiners.

I understand that my thesis may be made electronically available to the public.

Abstract

The characterization of functionalized cationic starch nanoparticles (StNPs) was conducted in this study. Three different strategies in the preparation of sustainable and biodegradable active packaging materials were explored. These strategies are: (1) to improve wet and dry strength by optimizing the composition of the pulp paper; (2) to introduce an antimicrobial component to the pulp using silver nanoparticles (AgNP); and (3) to explore paper sizing using hydrophobically modified starch. Firstly, cationic StNPs were used in combination with long or short cellulosic fibers (LCF and SCF) to enhance the dry and wet tensile strength of the pulp hand sheets. It was found that the wet and dry tensile index could be enhanced by 35% and 106%, respectively, over unmodified hardwood pulp. Additionally, it was found that the amount of SCF in the system correlated with the time it took to form the hand sheet in the filtration apparatus. The StNPs alone had no effect on the filtration time, but an increase in filtration time was observed when combined with SCF. It was observed that the hand sheets retained most of their tensile performance after undergoing repulping to reform the hand sheet.

Secondly, a method for introducing AgNPs into the pulp matrix to prepare antimicrobial hand sheets was evaluated. A green synthesis route was employed using tannic acid (TA) coated StNPs to reduce and stabilize the AgNPs. The size of the AgNPs could be altered by adjusting the concentration of TA and StNPs. The smallest AgNPs were observed for the highest concentrations of both TA and StNP. AgNPs impregnated hand sheets were prepared via the wet-end (pulp slurry) or dry-end (formed hand sheet) addition of the silver ions. Four different hand sheets were tested and compared with the control sample; namely the wet-end addition, dry-end addition

with two different concentrations of $AgNO_3$, and finally hand sheets containing only TA coated StNPs. All the hand sheets displayed enhanced antimicrobial activity for both *E. coli* and *S. aureus,* with the hand sheets prepared with AgNPs added in the dry-end step possessed the highest activity. These hand sheets also showed an increased tensile strength over the control for both wet and dry strength. The wet-end addition hand sheets had a reduced water vapour transmission rate (WVTR), while the other hand sheets showed an increased WVTR over the control sample.

Lastly, the sizing effect of the wet-end addition of water dispersible amphiphilic StNPs on pulp paper was demonstrated. Hand sheets produced using amphiphilic StNPs were able to temporarily repel water for several seconds and possessed a contact angle greater than 90°; a threshold for hydrophobic system. These hand sheets displayed increased dry tensile strength with no change in the wet strength. Additionally, these hydrophobic forces had no impact on the drying rate of the hand sheets.

The use of active packaging components will help reduce the negative influence of food waste on the environment by extending the shelf-life of perishable food products. Moreover, as the world recognizes the negative impact of using non-renewable materials and non-biodegradable plastics that accumulate in landfills and oceans, this work will offer a sustainable solution in the field of advanced packaging materials.

Acknowledgements

First, I would like to express my appreciation to my supervisor, Professor Michael K.C. Tam for his excellent support and guidance during my time here at the University of Waterloo. He believes in my abilities and provided me with the opportunity to demonstrate them.

I would like to thank Dr. William Anderson, Dr. Boxin Zhao, Dr. Juewen Liu and EcoSynthetix Inc. for providing the materials and access to equipment necessary to perform the tests for this research. Furthermore, I would like to thank my committee members, Dr. Boxin Zhao and Dr. Michael Pope, for taking the time to evaluate my thesis.

I would like to show my gratitude to all my lab mates who made working in the lab a fun and exciting experience. Additionally, I would like to acknowledge Drs. Yao, Shi, Mohammed, and Tanvir for their involvement in this project, as well as the contributions from the students that worked alongside me on this project: Daniel Lee, Caryn Hsiung, Andy Yang, Derek Li, and Ran An.

Finally, my family and friends deserve a very special thank you for their loving support and kindness throughout my journey. I definitely could not have made it here without them.

Table of Contents

List of Figures

List of Tables

Chapter 1: Introduction

1-1 Research Motivation

1-1.1 Current State of Plastic Waste

“We calculate that 275 million metric tons (MT) of plastic waste was generated in 192 coastal countries in 2010, with 4.8 to 12.7 million MT entering the ocean.” [1] This estimate was documented in a study by Jambeck et al. and it offers a brief insight into the current state of plastic waste around the world. In a 2017 report by the Ocean Conservancy [2], it was reported that food wrappers were the fourth most collected waste found on the beaches around the world with 762,353 articles of waste. They also found that plastic packaging (not including water bottles) was the tenth most collected item along the US coastline. Ocean borne trash does not always end up on the coastlines, instead much of the debris accumulate in oceanic gyres which can have hundreds of thousands of pieces of debris per square kilometer coming from worldwide sources [3], [4].

However, the total amount of plastic waste isn’t the main issue that is causing problems. The problem is what happens to the plastic after it leaves the hands of humans. The most common plastics used do not mineralize into carbon dioxide, water, and inorganic molecules [5]. Instead, many of these plastics end up in large bodies of water and breakdown into what is known as microplastics, which eventually are ingested by fish and bird species around the world [3], [6]–[8]. This results in many marine species suffering from suffocation, starvation, and toxins caused by the ingestion of these plastics [9]. A 2016 study by Miranda et al. [9] found that a small sample of commercial fish caught near the city of Salvador, Brazil contained microplastics. Since these are commercial fish, destined for human consumption, this

suggests that toxic substances within the plastic can enter the human food chain resulting in the bioaccumulation of various synthetic compounds that may have a negative impact on human health.

There are several ways to tackle the issues surrounding the widespread pollution of plastic wastes. These include more frequent cleanup efforts, stricter polluting policies, or finding ways to safely decompose the plastics. These methods offer a short-term solution to the challenges resulting from the use of synthetic plastic packaging materials. Longer term solutions require the elimination of the use of non-biodegradable plastics and moving toward more sustainable, biodegradable materials. To achieve this, researchers need to develop new processes, use alternative materials, and design products for consumption, but also address the issues surrounding their disposal. This perspective is best represented by Friege [10] in Figure 1-1 below.

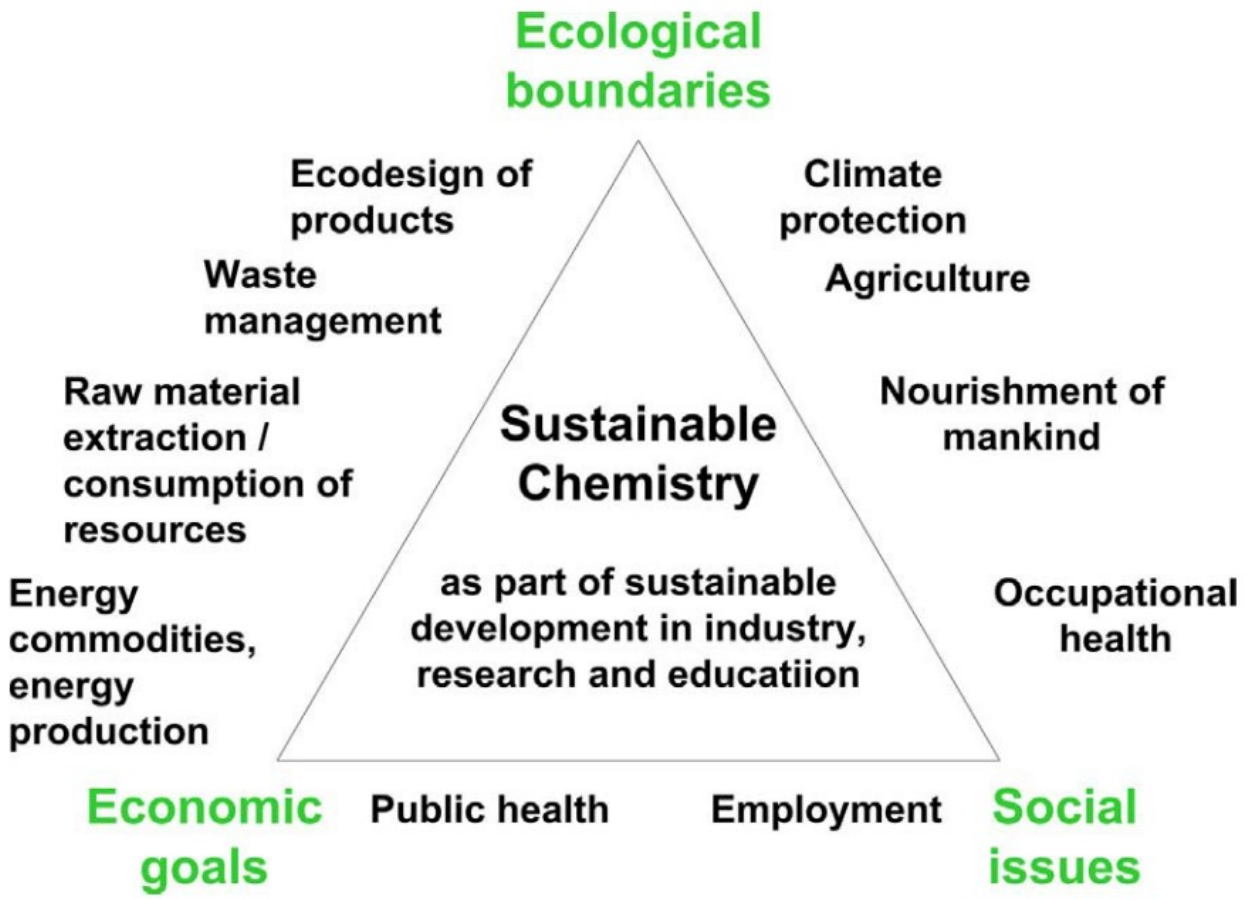

Figure 1- 1: Sustainable Chemistry interfaced with other global issues. (Taken from Friege, H [10])

1-1.2 Current State of Food Waste

In a 2014 report by Gooch and Felfel [11], it was found that, in Canada, almost 50% of food waste is generated at the household level as shown in Figure 1-2. This is estimated to cost $14.6 billion when accounting for the cost of producing, managing, transporting, and disposing of food products.

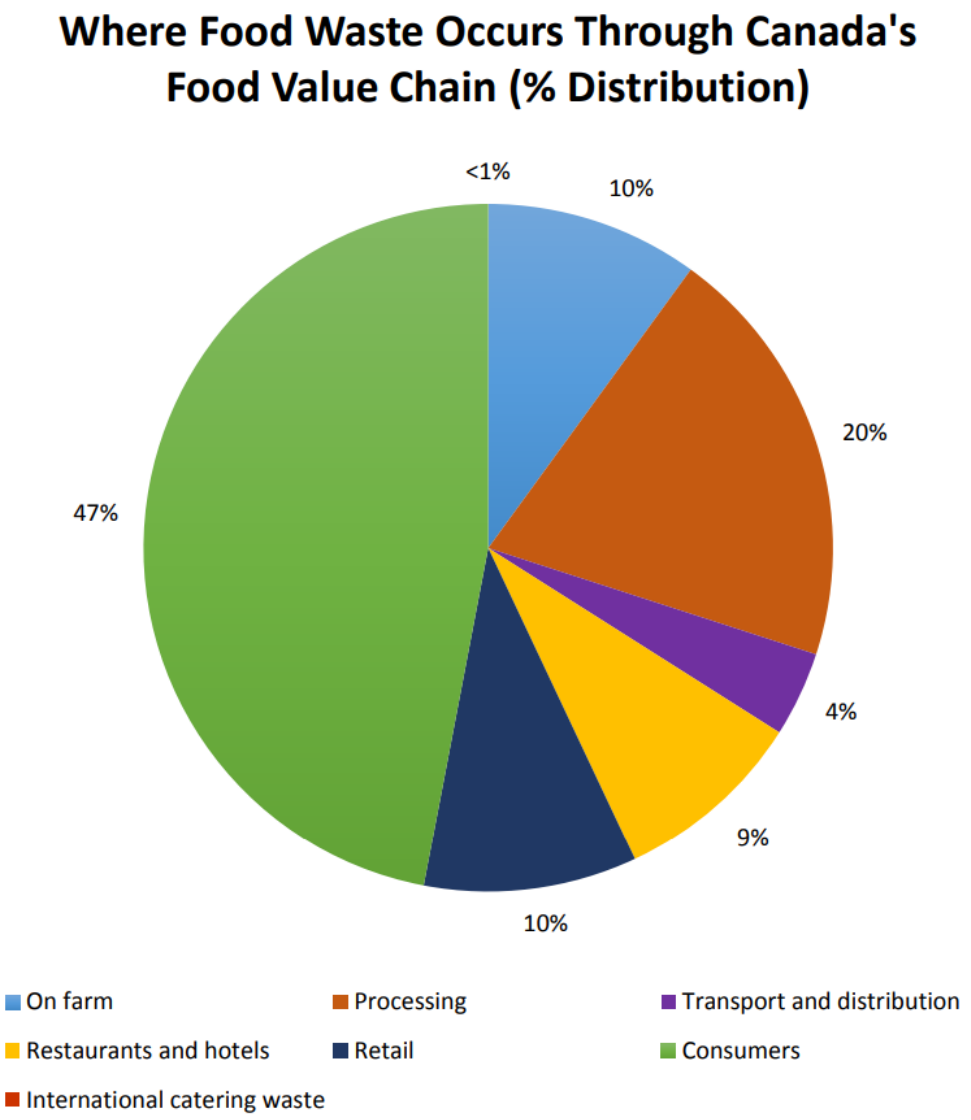

Figure 1- 2: Where food waste occurs through Canada's food value chain. (% Distribution) (Taken from Gooch and Felfel [11])

Additionally, in a 2017 report by the Commission for Environmental Cooperation (CEC) [12], it was estimated that, annually, the socio-economic impacts of this waste in North America accounts for:

- “193 million tonnes of greenhouse gas (GHG) emissions of carbon dioxide equivalent (CO_2 e) for life-cycle of landfilled [food loss and waste];
- 17.6 billion cubic meters (m^3) of water used;
- 22.1 million hectares (ha) of cropland used;
- 3.94 million tonnes of fertilizer used;
- 13.3 x 10^{18} Joules of energy used;
- 38.6 million m^3 of space used in landfill;
- US$1,867 million spent in tipping fees;
- US$278 billion in market value of [food loss and waste] lost;
- US$319 million–equivalent in loss of biodiversity; and
- 217 trillion kilocalories (kcal—1,000 calories) in potential energy lost.”

A large part of this waste is associated with food spoilage or exceeding their expiration date. While, there are dozens of methods to reduce the amount of food waste, that range from the farmer level to the consumers level as listed in the CEC report. One method is the prevention or delay of food spoilage by actively inhibiting mold and bacterial growth on the food through the use of active packaging systems [13], [14].

1-2 Research Objectives

The research described in this thesis is divided into three sections that address the challenges discussed in the previous section.

1-2.1 Tensile Enhancement with Starch Nanoparticles and Cellulosic Fibers

The first study examines the optimal composition of starch nanoparticles, pulp and cellulosic fibers in order to improve the tensile strength of the pulp paper. The tensile index of hand sheets was the key parameter used in the optimization of the formulations. Additionally, the filtration time, zeta potential, and repulpability of the hand sheets were examined in order to further understand the mechanisms of the starch nanoparticles, as well as, the processing challenges associated with the use of these components.

1-2.2 Antibacterial Enhancement with Silver Nanoparticles

The second study seeks to develop a method of incorporating silver nanoparticles into the pulp paper matrix in order to impart antimicrobial properties to the pulp paper. This methodology first examines the use of green chemicals, such as tannic acid and starch nanoparticles to synthesize and stabilize the silver nanoparticles. The size of the synthesized nanoparticles was optimized by adjusting the concentrations of tannic acid and starch. After this, the method to attach these nanoparticles to the hand sheet was evaluated. These hand sheets were examined for their antibacterial efficacy, tensile performance, water vapour transmission rate, and thermal decomposition in order to further understand the distribution and state of the silver nanoparticles in the hand sheet.

1-2.3 Hydrophobic Enhancement with Amphiphilic Starch Nanoparticles

The third and final study examines the impact of water dispersible amphiphilic starch nanoparticles on the sizing of pulp hand sheets. Surface tension measurements of the starch, drying rate of hand sheets, tensile strength and the dynamic contact angle of the hand sheets were examined to understand the hydrophobicity of starch nanoparticles in the hand sheet and their impact on the mechanical properties.

1-3 Thesis Outline

The thesis is organized into 6 chapters. Chapter 1 provides information on current real-world problems and motivation of the research. Chapter 2 provides a literature review of recent and relevant studies related to the materials used and goals of this thesis study. Chapters 3 through 5 examines the three research objectives, with one objective discussed per chapter. Finally, Chapter 6 displays the conclusions, recommendations and future work.

Chapter 2: Literature Review

2-1 Active Packaging

Active packaging (AP) has been gaining popularity over the last couple of decades, and the most recent year has had the most publications using this keyword. The term “active packaging” may be used to describe a type of packaging that can improve the shelf life of food in addition to, what is provided by an inert barrier to the external environment [13], [15]. AP should not be confused with intelligent packaging which is not related to improving the shelf life of food, but instead provides information to a consumer on the current state of the food beyond what the consumer can interpret from their own assessment.

Within AP systems there exists a subgroup of antimicrobial AP that are designed with a specific desire to inhibit or eliminate microbial growth, thereby providing a safer product to the consumer. Appendini and Hotchkiss [14] and Kerry et al. [16] provided extensive reviews on the subject of antimicrobial AP systems, and this was updated recently in a review by Ahmed et al. [17] for meat products. In these reviews, the types of AP are separated by the method in which the active agent is added to the system and performs its active role as shown in Figure 2-1.

Reviews on AP systems focus on three key repeating themes on the prospective trends and future research potentials. The first is related to health [17]–[23] and how the active agents will affect the food and ultimately human consumption. They also discuss concerns over how the packaging will affect the environment as these agents accumulate in our ecosystems. The second major theme is the economic viability of the advanced packaging systems [17], [19], [24], [25]. Having additional features added to the packaging systems increases the cost of production. The economics of balancing

the additional costs with the value of products preserved by these features can be a challenging task. The third and final theme is on the use of renewable resources in the packaging material [17], [26], [27]. The rapid development of renewable and bio-based materials is required to combat the effects of climate change and achieve a more sustainable future.

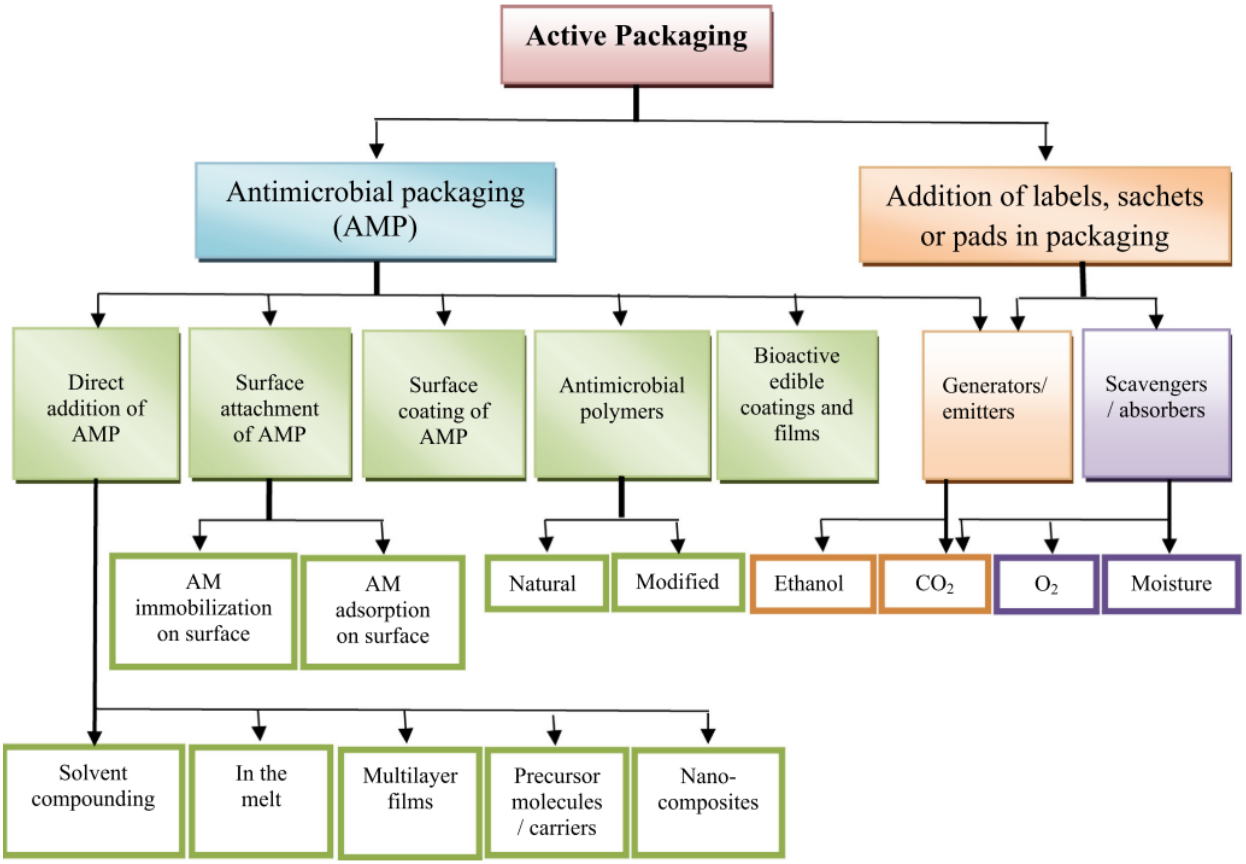

Figure 2- 1: Types of AP systems. (Taken from Ahmed et al. [17])

2-2 Antimicrobial Silver Nanoparticle Mechanism

One of the most popular and well researched antimicrobial active agents is silver and silver-based compounds. The majority of commercially available products in

antimicrobial AP for meats contain silver as the active component [26]. Metallic silver nanoparticles (AgNPs) are one subset of the available types of silver used for antimicrobial purposes. The biocidal mechanism of AgNPs has been extensively studied and it is still not completely understood. Currently, it is believed to be associated with the binding to DNA, the production of reactive oxygen species and damage to the cell membrane [28]–[35]. Since these associated effects are also commonly associated with the silver ion, it can be argued that the biocidal effects of AgNPs are due mostly to the oxidative dissolution of AgNPs to silver ions via the following reactions [33]:

$$4\,\mathrm{Ag}^{(0)} + \mathrm{O}_2 \rightarrow 2\,\mathrm{Ag}_2\mathrm{O}$$

$$2\,\mathrm{Ag}_2\mathrm{O} + 4\,\mathrm{H}^+ \rightarrow 4\,\mathrm{Ag}^+ + 2\,\mathrm{H}_2\mathrm{O}$$

Due to the fact that oxygen is necessary for the dissolution of metallic silver, Xiu et al. [33] reported that AgNPs had no inhibitory effects on *Escherichia coli* (*E. Coli*) under anaerobic conditions. It was also reasoned that the size effects of AgNPs could be associated with a more rapid release of ions from smaller nanoparticles, rendering them more toxic. Other reports based on the efficiency of AgNPs against its ionic forms, such as highly soluble silver nitrate, $AgNO_3$, or the relatively insoluble silver chloride, AgCl. Lok et al. [32] tested the antibacterial action of AgNPs and $AgNO_3$ on *E. coli* and found that AgNPs displayed similar antibacterial modes of action as $AgNO_3$. They also found that 1 nM and 1 μM of AgNPs and $AgNO_3$, respectively, were needed to extract the same level of bacteriolysis. Choi et al. [30] found that 1.4 μM of AgNP, AgCl, or $AgNO_3$ exhibited similar inhibition rates; about 10%. When the concentration is increased to 4.2 μM silver, $AgNO_3$ displayed 100%, but AgCl and AgNP were only half as effective. These tests were conducted at concentrations lower than the maximum

AgCl solubility, therefore the ionic concentrations, and thus inhibition rates, of $AgNO_3$ and AgCl should be identical. This point, however, was not addressed in the paper. A more definitive result of comparing silver ions against silver nanoparticles was reported in a paper by Ivask et al. [34]. By testing gene deletion mutants of *E. coli,* it was found that cells that were missing genes associated with cell surface antigen activity were notably more susceptible to inhibition from AgNPs than silver ions from $AgNO_3$. They also showed that the concentration required for *E. coli* inhibition was three times higher for AgNPs than for $AgNO_3$, and that intracellular silver ions were a better predictor for *E. coli* inhibition. Overall, these results suggest that there are many factors that impact the antibacterial activity of AgNPs and that determining whether AgNPs or silver ions is more effective should be determined on a case-by-case basis.

2-3 Starch Nanoparticles

Starch is cheap, renewable, biocompatible, and easily functionalized, making it an ideal building block for developing a sustainable system [36]–[38]. Naturally occurring starch is a large macromolecule comprised of glucose monomers with crystalline and amorphous domains that form large starch granules as shown in Figure 2-2 [39].

While starch has been used for many years, nanocrystal or nanoparticle starches (StNPs) are a recent development and the preparation and application of these particles is still being examined due to its unique and unpredictable properties when compared to macroscale starch. Changes to the rheological behaviour, thermal properties, and

solution stability are just some of the characteristics that can change dramatically depending on the surface chemistry of the starch, and how they are produced [40]–[42].

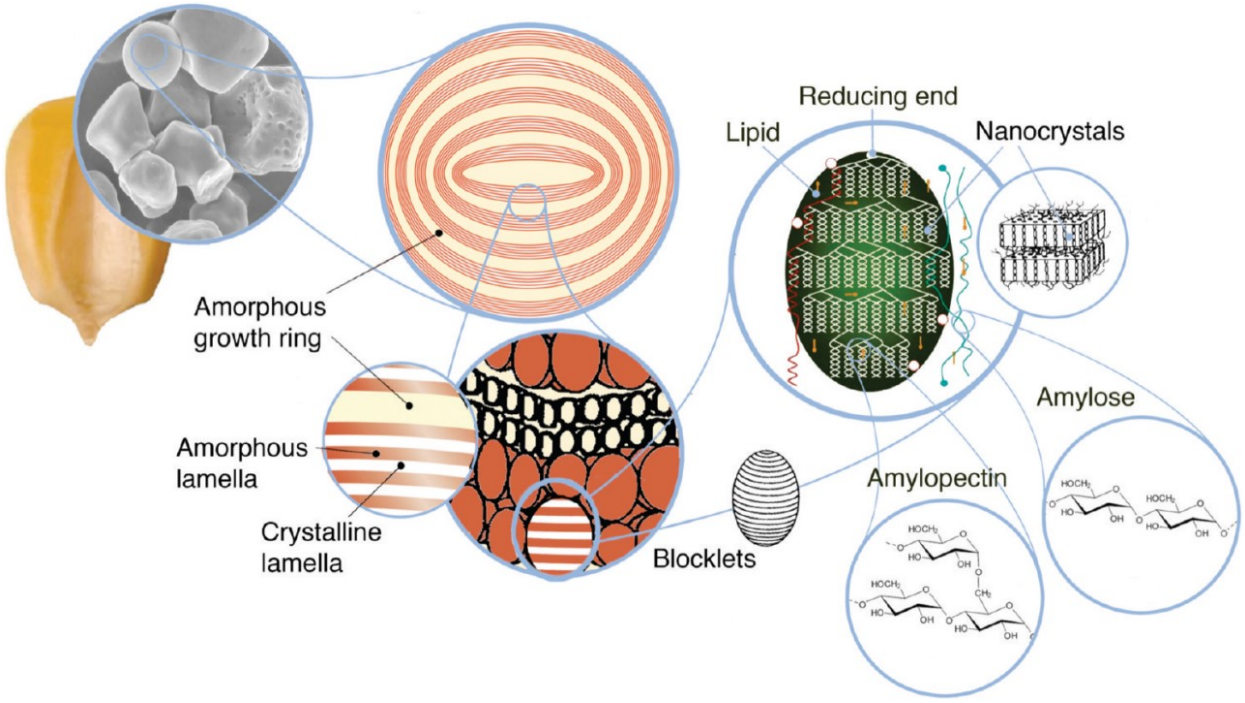

Figure 2- 2: An image showing the structure of starch nanocrystals and where they can be found naturally. (Taken from Šárka and Dvořáček [39]**)**

StNPs can be prepared through many methods, the most common of which are acid hydrolysis, nanoprecipitation, micro-emulsions, and, most recently, enzymatic treatment. Acid hydrolysis uses concentrated acid and long reaction times to disrupt the amorphous regions of starch granules resulting in starch nanocrystals. This method is relatively old, and several variations exist. Recent reports [43]–[46] generally cite three original sources reporting on the preparation of StNP by acid hydrolysis, namely Angellier et al. [47], Robin et al. [48], and Shaabani et al. [49]. Nanoprecipitation is a

recent method, where ethanol is used to gelatinize and precipitate starch while under vigorous mixing, which is then recovered by centrifugation. The nanoprecipitation procedure commonly cited in recent reports [50]–[52] is the one developed by Hebeish et al. [53]. StNPs are prepared within micro-emulsions by cross-linking of the polymer chains to induce precipitation, where the particle size is controlled by the characteristics of the micro-emulsions. This procedure has been used recently [54]–[58], and the procedures developed by Ding et al. [59], or Huang et al. [60] were cited. Finally, enzymatic treatment is the most popular procedure [40], [52], [61]–[65], as it is a recent development by Sun et al. [66]. This process is similar to acid hydrolysis, but the reaction time is significantly shorter and does not involve concentrated acids. Other less popular methods of producing StNPs include templates [67], ultrasonication [68], [69], and mechanical grinding [45], [70].

Recently, StNPs were used in a wide variety of applications, such as in drug delivery [44], [51], [53], [56], [57], [60], [62], [67], [69], algae flocculation [54], tissue engineering [58], fluorescent sensor [71], heavy metal adsorbent for wastewater [63], freestanding film [43], [64], stabilizers for Pickering emulsions [45], [52], digestion resistant starch or texturizing for food [55], [59], [65]. The applications of interest in the present study are to use the StNP as antimicrobial agents [61], [68], [72] in active packaging and as binder in papermaking [73].

2-3.1 Starch Nanoparticles used for Antimicrobial Applications

Qiu et al. [61] used starch as a template for loading menthone via the nanoprecipitation method. In this method, a loading capacity of up to 0.19 mL menthone / g of sample were achieved. The loaded StNPs possessed a slow release

profile of menthone that displayed antimicrobial activity against *E. coli* and *S. aureus*, as well as radical scavenging.

A similar study by Liu et al. [68] used peppermint oil loaded starch instead of menthone. Although a large component in peppermint oil is menthone and menthol, trace amounts of other compounds are present, [74] which may lead to differing results for the two studies. Liu et al. prepared StNPs via ultrasonication in the presence of peppermint oil to encapsulate the oil within the particles. The loading capacity of these samples was as high as 25.5 wt.% of oil in the StNP. Approximately 25-30% of the oil was released in 80 °C water within the first 2 hours and plateaued after that. A model fitted to the data predicted a maximum release of one of the particles to be about 33%, indicating that about 67% of the peppermint oil was permanently trapped within the StNP. The antimicrobial properties of these StNPs were not discussed, but, given its similarity to the study by Qiu et al., it would be interesting to examine the effectiveness of this system against bacterial growth.

Abreu et al. [72] studied a nanocomposite containing AgNPs and cationically modified montmorillonite clay to produce films for packaging. First, clay and starch were ultrasonicated to yield a dispersion, and then silver nitrate was added, which was reduced to metallic silver in the presence of sodium borohydride. The film was then prepared by evaporating 25 mL of the prepared solution on a glass plate. The contact angle, gas permeability, antimicrobial activity and contact test of the films were determined. Clay was found to increase the hydrophilicity of the films due to its high polarity while some mixtures of AgNPs significantly increased the hydrophobicity of the films yielding a contact angle of up to 82.8°. The gas permeability decreased

significantly with the inclusion of either clay or AgNPs. The lowest permeation rates attributed to the presence of clay and AgNPs were $1x10^{10}$ g O_2 /m-s-Pa and $9x10^9$ g H_2O /m-s-Pa, respectively. The antimicrobial activity was determined from the inhibition zones for *C. albicans* (yeast), *S. aureus* and *E. coli*. Inhibition of growth for all three cultures was observed in the presence of AgNPs, while the clay was capable of only inhibiting the bacterial growth, but not the yeast. Finally, the contact test was used to determine the amount of material released from the film to a food simulant. This is critical to determine the safety of the product. The simulant used in this study was 3% acetic acid at pH 2.5 and 40 °C over the course of 10 days. For the films containing AgNPs, the highest measured value was 0.70 mg/g, which could be considered safe for food contact.

These works show the use of StNPs in antimicrobial applications. By using bio-based menthone or peppermint oil the reports by Qiu et al. and Liu et al. highlight the possibility for completely biodegradable antimicrobial StNPs that could be used for AP systems. Additionally, Abreu et al. shows how AgNP modified StNPs can be safely used for AP applications.

2-4 Tannic Acid

Tannic acid (TA) has been extensively used as a reducing agent to produce silver nanoparticles [75]–[79]. The use of TA is a result of its many desirable characteristics, such as antimutagenic, antimicrobial, antiviral, anticarcinogenic, anti-inflammatory and antioxidant properties [80]. The environmentally friendly TA can be used as both a reducing and capping agent to prevent the aggregation of AgNPs

produced. Cao et al. [75] reported on the optimal pH and TA concentrations to synthesize tuneable monodisperse AgNPs. At pH 6.0 the size of the AgNPs was about 44 nm due to slow reaction kinetics and a duration of two hours used to prepare the nanoparticle. However, at pH 8.0, the rapid nucleation of AgNPs led to a particle size of 10 nm and a fast reaction time of less than 1 minute. Increasing the ratio of TA/$AgNO_3$ up to 1.00 (maximum tested) resulted in the production of smaller particles due to the proportional increase in the rate of reaction. Fang et al. [76] used TA to synthesize and coat AgNPs and AuNPs, which were then tested for their corresponding antibacterial capabilities against *E. coli*. The nanoparticles were roughly 54 and 60 nm in size for AgNPs and AuNPs respectively. The minimum inhibition concentration (MIC) for the TA coated AgNPs at 48h was determined to be 100 μg/mL and that this same concentration could reduce 99% of the *E. coli* population within 5 hours. However, pure TA displayed no antibacterial properties on *E. coli*. Kim et al. [77] prepared AgNPs with a hydrodynamic size of 47 nm using TA at a temperature of 85 °C. The antibacterial analysis was tested against 22 strains of 8 types of bacteria. The most common, and lowest MIC reported in this study was 6.74 μg/mL Ag with 21.26 μg/mL TA. This MIC value was effective against 15 of the 22 strains tested and it was found to be more effective against gram-negative bacteria than gram-positive bacteria. Ranoszek-Soliwoda et al. [78] compared the use of TA and citric acid (CA) as reducing and capping agents for AgNPs. It was observed that TA produced polydispersed spherical AgNPs while CA produced a wide variety of sizes and shapes. When TA and CA were used together (as a TA-CA complex), monodispersed AgNPs were produced. The

mechanisms of reduction were examined using voltammetric measurements, FTIR and computer modelling.

The mechanism of reduction is accepted to be the oxidation of the many catechol groups present on the tannic acid to quinones under alkaline conditions as reported by Fang et al. [76] in Figure 2-3 and Ranoszek-Soliwda et al. [78]. This is related to the mechanism reported for polydopamine catechol groups as well [76], [81].

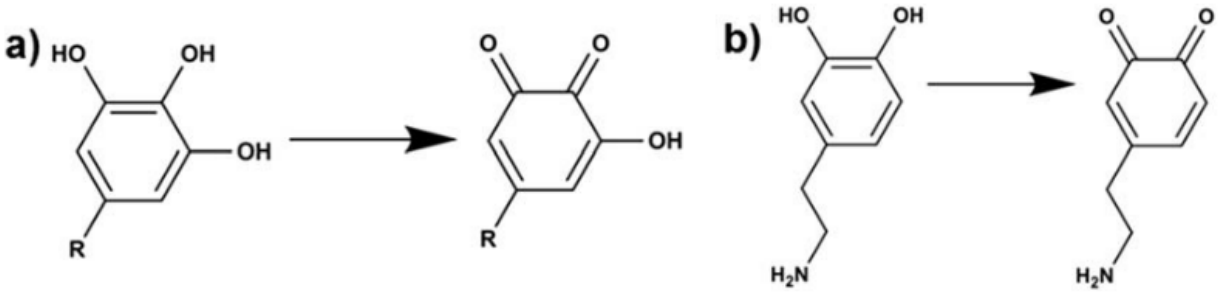

Figure 2- 3: Oxidation of catechol groups from a) TA and b) dopamine into quinone groups before polymerizing. (Taken from Fang et al. [76]**)**

TA is known to self-polymerize under slightly alkaline conditions, this polymerization reaction has been used to coat surfaces with TA. This reaction is related to the polymerization of dopamine in alkaline conditions involving covalent and non-covalent bonds of benzene rings. [82]–[84].

2-5 Paper Sizing with Modified Biopolymers

Sizing refers to the addition of components to a paper composition to resist the permeation of liquids into paper fibers. Two widely used and well-studied paper sizing agents are alkenyl succinic anhydride (ASA) and alkyl ketene dimer (AKD). They are added during the wet-end of the paper formation and heated to over 100 °C to promote

a reversible reaction with the cellulosic pulp [85]. Both ASA and AKD hydrolyze in water, thus they require a stabilizer, such as cationic starch, to slow this hydrolysis [86]–[88]. Recent literature reported on the combination of hydrophobic reagents with biopolymers in the preparation of films [89], [90], polymer blends [91], hand sheets [86], [87], [92], as a coating [88], [93], [94], or as hydrophobically modified powders [95], [96].

Winkler et al. [89] produced fatty acid modified starch esters to prepare casted films. They changed the length of the fatty acid to examine the effects on the films' mechanical, hydrophobic, structural and thermal properties. They showed that increasing the chain length and degree of substitution resulted in more "oil-like" films that were more hydrophobic, possessed lower strength and Young's modulus, and higher crystallinity. The contact angle of the films ranged between 95° for the hexanoate modified starch films, to about 107° for the stearate modified starch films. Muscat et al. [90] prepared starch and wax composite films with glycerol and Tween-80 additives; which assist in the processing. Three different types of waxes were studied (beeswax, candelilla wax, and carnauba wax) at two different concentrations (5%, 10% w/w). The casted gelatinized starch films were tested for mechanical, barrier, structural, optical, thermal, and hydrophobic properties. The highest contact angle reported in this study was 87.6° for the 5% carnauba wax film containing Tween-80. Interestingly, in the absence of Tween-80, the contact angle decreased to 48.6°. This effect was attributed to the roughness of the films and how Tween-80's self-assembly behaviour depended on the type of wax used.

Polymer blends of starch and gelatin were prepared by Acosta et al. [91] using glycerol as a plasticizer. Additionally, the blends contained mono- or di-esters of

glycerol fatty acids at 15 wt.%. The structure, barrier properties, mechanical, and optical properties were studied, and gelatin was responsible for increasing the stiffness and strength of the casted polymer blend films, whereas the fatty acids reduced stiffness and increased elasticity. The water permeability of the films was reduced in the presence of fatty acids, but the oxygen permeability was increased. Films containing fatty acids maintained better mechanical properties after 5 weeks of storage over those that did not have fatty acids.

Kumar et al. [86] prepared hand sheets using ASA stabilized by cationic starch and polyvinylamines (PVAs). The hand sheets contained additional additives, such as cationic fixing agents (fatty acid condensation product), cationic electrolyte (poly aluminum chloride) and a retention aid (cationic polyacrylamide). It was found that hand sheets prepared with cationic starch possessed a contact angle of about 110° when the emulsion was used immediately. However, the contact angle decreased to below 60° after 1 hr. Alternatively, the hand sheets prepared with the PVA emulsion maintained a constant 110° contact angle after 4 hours, but this decreased substantially afterward. Sun et al. [87] also prepared hand sheets using ASA emulsions that were stabilized with cationic starch and cationic modified cellulose nanocrystals (CNCs). This emulsion was added to a mixture of hardwood and softwood pulp at a 7:3 ratio. Other additives that were used include poly aluminum chloride, precipitated calcium carbonate, CatioFast® and Percol®. Hand sheets prepared with the starch and CNC stabilized emulsion displayed a contact angle of around 111° when used immediately. This contact angle decreased to 108° after 6 hours of storage. The emulsions prepared without starch or CNC possessed a contact angle range between 110° (0 hours) and 103° (6 hours).

These hand sheets also displayed a tensile index of about 55 Nm/g, which was independent of storage time. Finally, hand sheets prepared by Yuan et al. [92] were prepared using bacterial cellulose, cationic starch and cationic polyacrylamide (CPAM) with AKD as the sizing agent. Chitosan and polyamideamine-epichlorohydrin (PAE) were also used to improve the sizing effects. It was found that bacterial cellulose had a negative effect on the degree of paper sizing, as it would preferentially bind to the AKD due to its surface area and charge resulting in the loss of both components through filtration. They also showed that cationic starch and CPAM were able to individually increase the sizing degree, but they worked best when used together. Additionally, PAE and chitosan were able to improve the sizing degree of the paper by forming cationic bridges between the negatively charged AKD and negatively charged pulp fibers, though the order of addition during the paper production process could alter the sizing results.

Hydrophobic paper coatings, where sizing agents were not added during the wet end, were prepared by Dang et al. [88]. In the study, non-crystal microporous starch was reacted with AKD and then applied to softwood kraft pulp using a drawdown rod. The optimal reaction conditions between the AKD and starch were evaluated, and the sized papers possessed excellent hydrophobicity (not quantified) over the control. This effect was attributed to the porous structure being filled by the hydrophobic starch as confirmed by SEM images. Guazzotti et al. [93] prepared coatings for paperboard using purely gelatinized starch with and without the addition of D-sorbitol. In this case, the migration of long alkanes (C_{18} – C_{28}) through the coating was studied instead of water, and the coated paperboard resisted the migration of alkanes as confirmed by HPLC-

GC-FID analysis. Calce et al. [94] coated polyethylene films with fatty acid modified pectin. While barrier properties against water were not studied, the antimicrobial and oxygen scavenging ability were evaluated. Coated polyethylene was capable of resisting bacterial growth of *E. coli* and *S. aureus*, and fatty acid modification yielded about 60% inhibition for both bacterial types. Due to the double bonds found in oleic and linoleic acids, oxygen concentration within the coated polyethylene film decreased over time.

Cova et al. [95] prepared hydrophobic powders by reacting cassava starch with octenyl succinic anhydride (OSA), as well as, carboxymethylated cassava starch with quaternary ammonium salts. They tested the moisture sorption isotherms and found that the OSA modified starch did not absorb as much water as the unmodified starch. The data was fitted to a model and the parameters were compared to determine the optimal reaction conditions for reducing the moisture sorption. Wei et al. [96] prepared starch nanocrystals modified with hexadecyltrimethoxysilane (HDS) by covalent bonding of HDS to the starch to impart hydrophobic characteristics. The contact angle of the powder was measured by first forming a pellet under a hydraulic press. The pellet displayed a contact angle of 119° compared to 43° for the native starch. The hydrophobic powders were capable of dispersing in polar and non-polar solvents, such as n-hexane, tetrachloromethane, chloroform, acetone and water. However, after some time the particles would aggregate and precipitate.

Overall, these studies show some recent developments in the hydrophobic modifications of starch to produce water repelling films or polymer blends, as well as, the use of starch as a major component in paper sizing

2-6 Comparison of Existing works

Many of the steps described in this thesis are based on the reported literature, therefore, it is necessary to differentiate the results reported in this study from previous reported studies. It is believed that, at the time that this thesis is written, the following list can be considered novel achievements from this research.

1. **The self-polymerization of TA in the presence of StNPs to reduce and stabilize AgNPs.** While the usage of TA to reduce and stabilize AgNPs and the self-polymerization of TA to coat surfaces has been reported, the effects of concentration and ratios of StNPs are new. These findings are useful for determining the optimal formulation for the green synthesis of AgNPs.
2. **The method of incorporating the above material into a pulp-paper matrix has been developed in this study**. While the process of incorporating additives to a paper matrix is not new, this is the first reported study on TA and AgNP modified StNPs. This work builds the foundation that allows for the advancement of sustainable active packaging materials.
3. **Using StNPs as pulp-paper filler to increase mechanical strength is thoroughly examined for the first time.** The use of StNPs as paper binders for paper coating has been previously reported, but it is deposited on pre-formed paper and not during the paper preparation from pulp. Moreover, the combined use of the StNPs with short and long fiber cellulosic material is new. To reduce the reliance of oil-based plastic packaging, the enhancement of paper strength is a necessary step that must be completed.

4. **The study of a water dispersible amphiphilic StNP for paper sizing is an original contribution.** Hydrophobically modified powders have been prepared but these powders were not introduced as a hand sheet additive. Alternatively, studies that had formulated hand sheet additives or paper coatings were prepared as a solution prior to use. Therefore, the effects of a ready-to-disperse powder for the preparation of hydrophobic hand sheets have not been reported. This novel powder will reduce the complexity of the paper making process by eliminating the need to constantly prepare ASA emulsions that degrade over time.

Chapter 3: Mechanical Performance of Starch Nanoparticles and Cellulosic Nanomaterials in Paper Products

3-1 Introduction

To move away from unsustainable oil-based plastics, the increasing use of paper-based products and packaging materials is considered an attractive alternative. A drawback in using pulp-paper is the loss of tensile strength when the packaging encounters water. This makes untreated pulp-paper unsuitable for some applications, such as fresh food packaging, where it would absorb moisture from the food product and disintegrate. Wetting of the fibers disrupts the inter-fiber hydrogen bonds, thus reducing the paper strength significantly [97]. Additives can be used to overcome these challenges and provide improved tensile strength performance over the base pulp. The papermaking industry uses many different additives to achieve these challenges [98], however this study will focus primarily on the use of biocompatible renewable materials, such as starch nanoparticles (StNPs), short cellulosic fibers (SCF), and long cellulosic fibers (LCF) [73], [99].

Starch is the most often used bio-material in papermaking [100]–[102], and it is used in its modified and unmodified forms. The modified forms can be used for paper sizing, to improve printability, to increase retention, or to enhance the smoothness of the paper [100], [103]. StNPs are promising materials that harness all these positive features from bulk starch and they exist as low viscosity suspensions even at high solids [73]. There are different methods to produce starch, with the most commonly cited being acid hydrolysis, nanoprecipitation, micro-emulsions and enzymatic treatment. However, this study uses StNPs prepared through a high yield, and little to no waste by-product, mechanical extrusion technique [42].

Microscale and nanoscale cellulosic fibers have recently been used as additives in papermaking to improve tensile strength [99], [104], [105]. These fibers operate by improving the fibre-fibre bonding via hydrogen bonds across pulp fibers, which act as part of a load-bearing network. Cellulosic fibers are also used as paper coating materials to reduce surface porosity leading to increased barrier properties and a smoother surface. However, these small fibers cause dewatering issues during the papermaking process, which limits the maximum amount of usable additive.

This study will examine the use of StNPs to improve the tensile performance when used in combination with SCF or LCF and the optimal concentrations to achieve the best results. These components have been studied individually, but the combined effects of the StNP with the cellulosic fibers have not been previously reported.

3-2 Experimental

3-2.1 Materials

Cationic starch nanoparticles (StNPs), hardwood pulp (HWp), and long cellulose fibers (LCF) (~1 mm length) were provided by EcoSynthetix Inc. (Burlington, ON, Canada). The StNPs are approximately 100-200 nm in diameter with a spherical morphology. Short cellulose fibers (SCF) (50 nm width, >100 μm length) were purchased from The University of Maine Process Development Center (Orono, Maine, USA).

3-2.2 Preparation of Hand Sheets

Hand sheet formation and preparation are based on procedures described in the TAPPI method T205 sp-02 with some minor modifications to accommodate the materials and equipment available for this study.

3-2.2.1 Stock Pulp Dispersion

The pulp dispersion was prepared by hand shredding 9.0 g of pulp (HWp) into small pieces that were approximately 1 cm^2. This was then added to 291 mL of deionized water (3 wt.%) in a steel mixing bowl, SUNBEAM 2379-33A. The dispersion was mixed at a speed setting 3 for 5 minutes while rotating the bowl to ensure homogeneity. From this, 300 mL of deionized water was added (1.5 wt.%) and mixed in a pneumatic mechanical stirrer for 30 minutes, such that a vortex was formed. After 30 minutes, 2.4 L of deionized water was added (0.3 wt.%) and mixed for another 60 minutes at the same speed. Finally, a lid was placed on the dispersion and stored at room temperature. Since the pulp settles rapidly, the dispersion was mixed for at least 15 minutes prior to use.

3-2.2.2 Additive Dispersion

To prepare the additive dispersion, the StNPs, LCF, or SCF were measured as necessary and then diluted to 0.1 wt.% solids with deionized water. The dispersion was then sonicated with an ultrasonic probe, MICROSON model no. XL2000, at room temperature until the StNP aggregations were no longer visible, approximately 10 minutes duration. This additive dispersion was stored for a maximum of one day prior to use.

3-2.2.3 Sample Dispersion and Hand Sheet Filtration and Drying

The sample dispersion was prepared using different amounts of additives. The hand sheets were prepared based on a final dry mass of 750 mg. For example, to prepare a 5% additive sample, 237.5 mL of the stock pulp dispersion was added to a beaker. This was then followed by the dropwise addition of 37.5 mL of the additive dispersion to prevent aggregation, and the dispersion was then mixed for 30 minutes.

After 30 minutes, 1 L of deionized water was added to the filtration module together with the additive dispersion. After approximately 5 seconds, a mild vacuum was applied to form the hand sheet on a 200-mesh steel filter (75 μm pores) with a diameter of 10 cm. The hand sheet was blotted with roughly 10 filter papers, WHATMAN 1 category no. 1001110 and 1001125. The blotted hand sheet was placed between two dry filter papers and then pressed with a hydraulic press, MOTOMASTER model no. 009-1096-8, at 50 psig for 5 minutes and then again for 2 minutes while replacing the filter papers in between presses. Finally, this hand sheet was placed in the oven at 80 °C for 24 hours to dry.

3-2.3 Tensile Test

Tensile tests were performed with a CETR-UMT (BRUKER). The tensile index is defined by TAPPI method T494 om-01 by the following equation:

$$TI\left(\frac{Nm}{gram}\right) = \frac{Tensile\ Strength\left(\frac{N}{m}\right)}{Grammage\left(\frac{grams}{m^2}\right)} = \frac{\left(\frac{F*g}{W}\right)}{\left(\frac{m}{L*W}\right)}$$

where F is the maximum force in kg as reported by the apparatus, g is gravitational acceleration constant, W is the width of the strip in meters (0.014 m), L is the length of the strip in meters (0.060 m), and m is the mass of the paper strip in grams.

The samples were prepared for tensile testing by cutting the hand sheets into strips of 14 mm x 60 mm. The distance between the clamps measured 40 mm, the elongation rate was 18 mm/min, and the test was performed at room temperature. The wet tensile strength was determined by adding 30 µL of deionized water to the center of the paper sample, the sample was loaded into the clamps as soon as the droplet had been completely absorbed into the paper.

3-2.4 Filtration Time

The filtration time was calculated using a frame-by-frame analysis of a video during the paper filtration process. To maintain the same testing conditions, the starting height of the pulp dispersion in the filtration apparatus was kept constant by diluting the dispersion, as necessary, with deionized water. Additionally, the outlet valve was open to atmosphere, instead of a vacuum to reduce the variables. At the beginning of the experiment this outlet valve was plugged with a stopper until the required height of water was achieved.

The length of time reported was the duration between the frame the stopper was removed from the outlet valve to the frame where the constant stream of filtered water turns into drops of water. The tests were performed in duplicate.

3-2.5 Repulpability of the Hand Sheets

Due to the ultimate usage of the tensile performance additives, it is necessary to probe the effect that two filtration cycles would have had on the tensile performance. First, to emulate industrially produced pulp sheets, a thick hand sheet, consisting of 6 times the normal dry weight (4.5 g), was prepared in the same manner as described earlier. This thick hand sheet was blotted and pressed normally. The thick hand sheet was dried in the oven at 80 °C until 10% moisture was reached, where it was then ripped by hand and added to the pneumatic mechanical stirrer at 0.3 wt.% solids until completely disintegrated. After complete disintegration the normal hand sheet preparation was used. The only composition tested for this experiment was a 5 wt.% addition level of StNP:SCF (1:1)

3-2.6 Characterization

Zeta potential measurements were performed using a MALVERN ZEN3690. The zeta potential measurements were done to determine the shielding effect of cationic StNPs on anionic SCF. The samples were diluted with DI water until the results were within the necessary count rate for accurate results.

3-2.7 List of Tested Samples

The following table shows samples that were prepared and the tests performed on them.

Table 3- 1: List of formulations tested

Additive Composition	Ratio	Addition Level Tested (Wt.% Total Dry Weight)		
		Tensile Test	Filtration Time	Repulping
StNP	-	1, 3, 5, 8, 10	5	
LCF	-	1, 3, 5, 8		
SCF	-	1, 3, 5, 8	2.5, 5	
StNP:LCF	1:1	1, 3, 5, 8		
	2:1	3, 5		
StNP:SCF	4:1	1, 3, 5, 8, 10		
	2:3	1, 3, 5, 8, 10		
	1:1	1, 3, 5, 8	5	5
	3:2	1, 3, 5, 8, 10		
	2:1	1, 3, 5, 8		
	1:4	1, 3, 5, 8, 10		

3-3 Results and Discussion

3-3.1 Preliminary Trials

Figure 3-1 shows the preliminary tensile trials quantifying the wet and dry tensile strength of the hand sheets formulated with StNPs, LCFs, SCFs, and combinations of StNPs with LCFs and SCFs. StNPs increased the dry tensile index by about 10 Nm/g (+35%) over the control at all compositions, which suggested a saturation of StNPs at a level as low as 1 wt.% by dry mass. This increase in dry tensile strength was reported in other studies using cationic starch [101], [102], [106]–[108]. The dry strength was attributed to the electrostatic binding of cationic StNP and anionic HWp [103]. The large surface area of the StNP could bind to HWp fibers, while two anionic fibers would naturally repel. For wet tensile performance, the tensile index decreased slightly with the addition of StNPs. In this case, the increased addition of StNPs resulted in further reduction in the wet tensile index. The decreasing trend was likely attributed to the

hydrophilic and swelling behavior of the cationic StNPs in the presence of water. This in turn disrupts the existing hydrogen bonds between StNP-HWp and HWp-HWp [109].

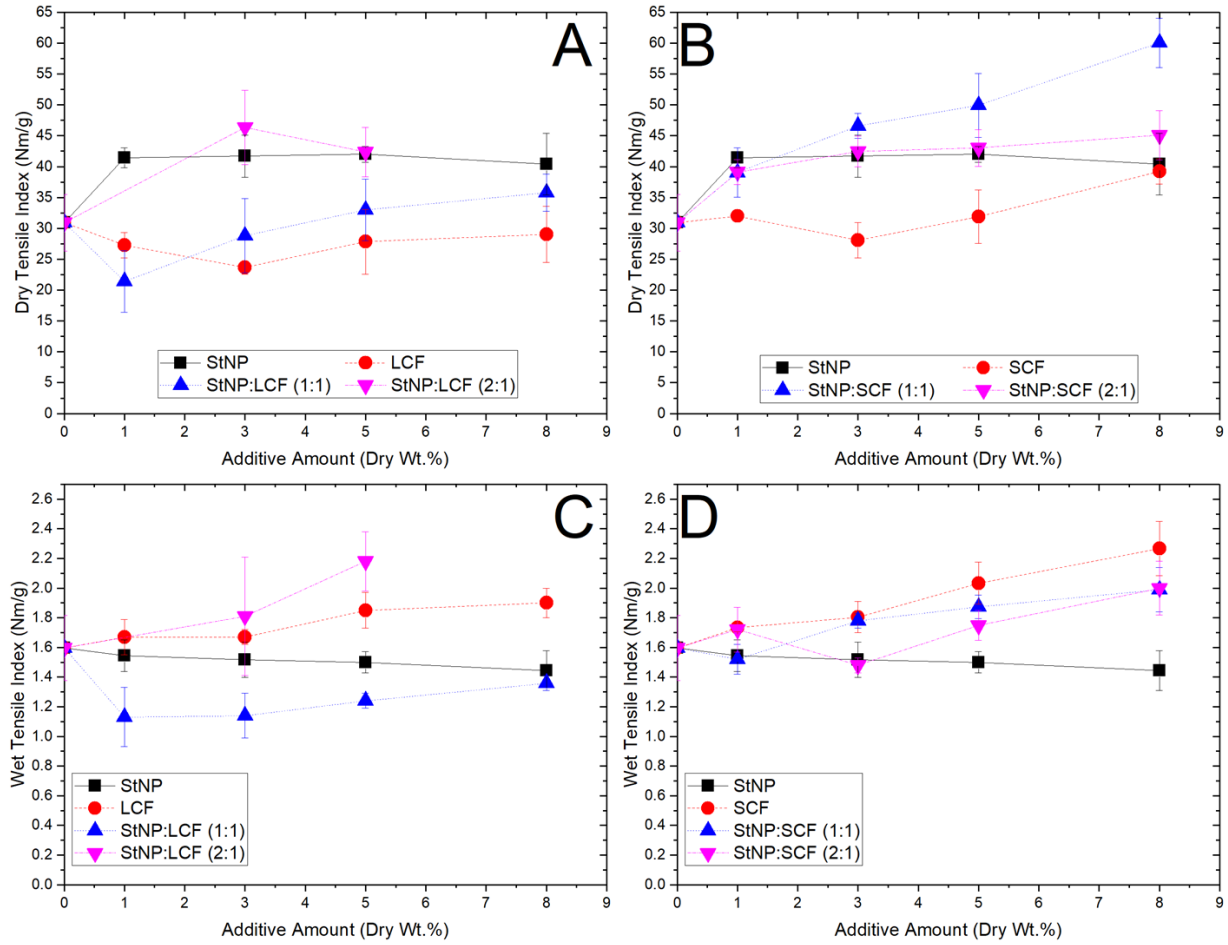

Figure 3- 1: Dry tensile index of StNPs and LCF (A) or StNPs and SCF (B) as well as wet tensile index of systems involving StNPs and LCF(C) or StNPs and SCF (D) at different addition levels

LCFs and SCFs displayed opposing trends to the StNPs, that is, the dry tensile index generally decreased or remained unchanged with the addition of LCFs and SCFs while the wet tensile index increased. The combined addition of these fibers with the StNPs resulted in the improvement in both wet and dry tensile strength. The most

significant impact was reported for the StNP:SCF at a composition of 1:1 since it possessed the highest overall increase over the control for wet and dry strength. Interestingly, when this ratio was changed to a 2:1 ratio of StNP:SCF, both the wet and dry strength decreased, which implied that the performance could be optimized by adjusting both the ratio and addition level of the StNP:SCF system.

3-3.2 Optimization of the StNP:SCF system

To determine the most ideal formulation, four new compositions were tested; 1:4, 2:3, 3:2, 4:1. Furthermore, these were tested up to a 10 wt.% addition level to examine if a maximum could be reached. The data from the preliminary trials was compared with the new results to obtain a complete picture for the optimization of the formulation as shown in Figure 3-2. In this case, the x-axis displays the total dry weight of StNPs or SCFs rather than the total additive amount. This emphasized the impact that the StNPs or SCFs had on the tensile strength of the hand sheets individually.

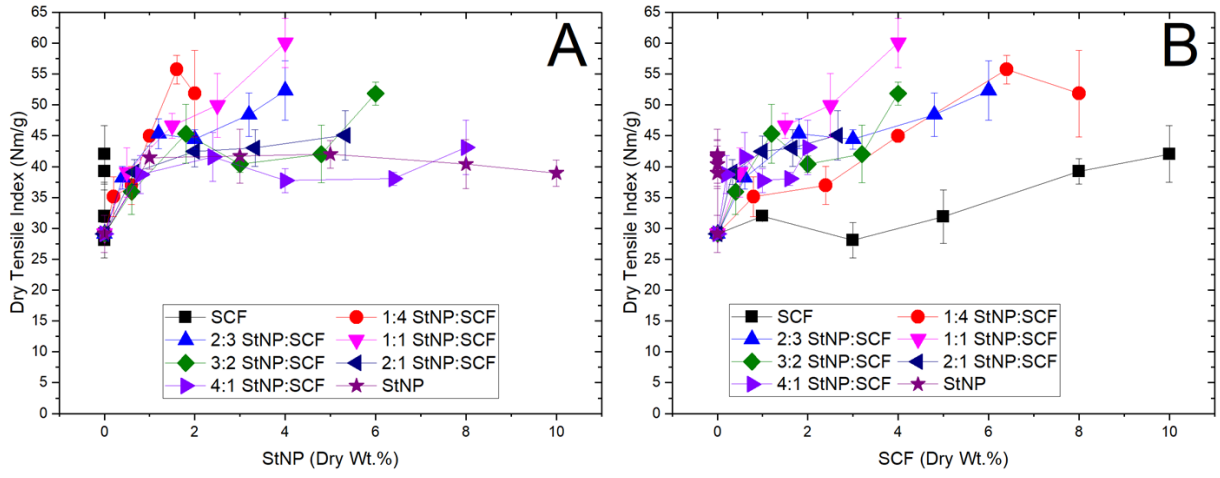

Figure 3- 2: Dry Tensile Index for different compositions of StNP (A) or SCF (B)

It can be seen that the dry tensile index approached a maximum at a 1:1 ratio of StNP:SCF at a 4 wt.% StNP amount (8 wt.% total additive) with a value of 60.06 Nm/g. Increasing or decreasing this ratio reduced the tensile index. Additionally, the dry tensile index of StNPs increased sharply until about 1 wt.% StNPs, where it remained constant. However, it continued to increase further with the addition of increasing amounts of SCF. In Figure 3-2B SCF displayed very little effect on the dry tensile index below 5 wt.% but the dry tensile index increased dramatically when a small amount of StNPs were added. Figure 3-3 shows the zeta potential measurements of StNP:SCF mixture, where the zeta potential of the anionic SCF became less negative as cationic StNPs were bound to the anionic surface. The coating of StNP on the exterior of the SCF promoted the charge interactions between the pulp fibers, resulting in an increase in its dry tensile strength.

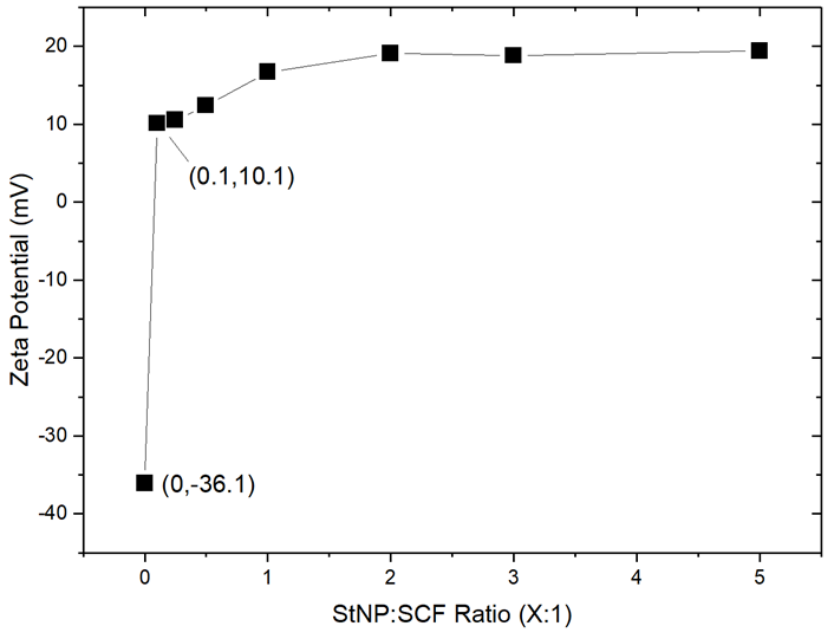

Figure 3- 3: Zeta potential of the StNP:SCF system at varying compositions

The wet tensile index trends differed from to the dry tensile index. As previously mentioned, the addition of StNPs decreased the wet tensile strength in the HWp control sample, whereas the SCF resulted in an increase in the wet tensile strength, which is clearly demonstrated in Figure 3-4

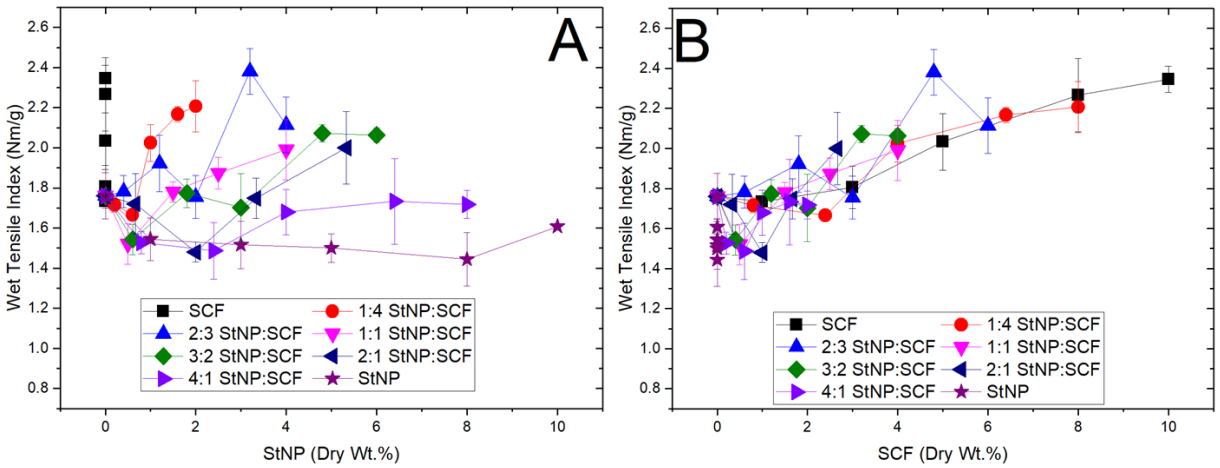

Figure 3- 4: Wet tensile index with respect to concentration of StNP (A) or SCF (B)

Wet tensile strength was strongly correlated to the amount of SCF present in the system. The addition of StNPs in the hand sheet composition was detrimental to the wet tensile index when the ratio of StNP:SCF was greater than 3:2. However, in Figure 3-4B it was observed that the 1:4, 2:3, 1:1, and 3:2 ratios of StNP:SCF followed the trend of SCF alone, suggesting that the addition of StNP had no effect on the wet tensile index as long as it was less than the ratio of 3:2. Thus, the ideal composition would therefore depend on whether the increased wet or dry strength is more desirable and the cost of the StNP and SCF materials. We concluded that small amounts of StNPs dramatically increased the dry strength, but it had little impact on the wet strength.

3-3.3 Filtration Time

The filtration time could have had a large effect on the rate at which the paper could be produced in a paper mill. Figure 3-5 summarizes the key findings; where the key relationships between the StNP and SCF were determined. Firstly, StNPs alone had no effect on the filtration rate of the pulp. However, with the addition of SCF, a large impact on the filtration time was observed, consistent with reported findings in the literature [104], [105]. At 5 wt.% SCF, filtration time was increased by about 9.5 seconds (+59%) over the control. The most interesting finding was that while StNPs alone had no effect on the filtration time, the 5 wt.% StNP:SCF (1:1) composition possessed a higher filtration time than the 2.5 wt.% SCF. This means that at the same total amount of SCF, the addition of StNPs had a combined effect on the filtration time by increasing it about 1.7 seconds (+8%) over the SCF alone. This combined effect was likely due to the coating of StNP on SCF that induced changes in the network structure of the pulp.

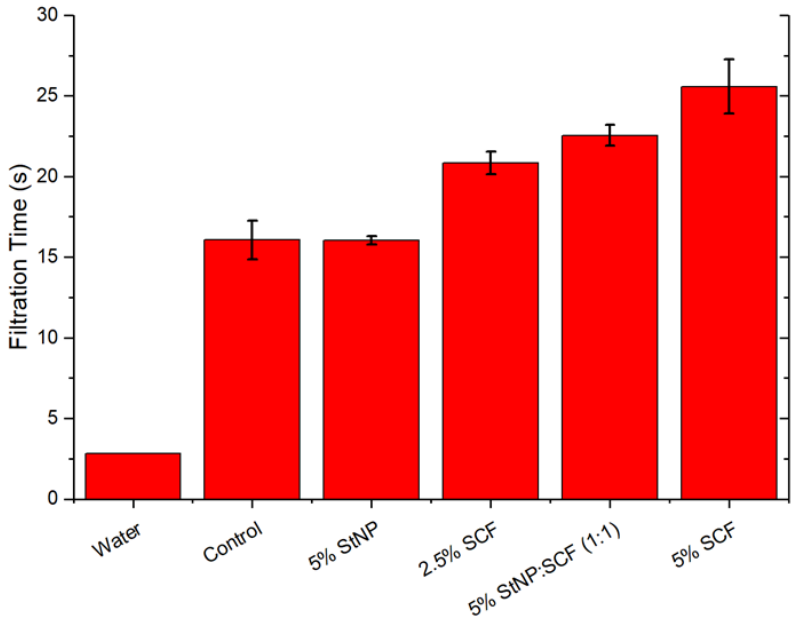

Figure 3- 5: Filtration time in seconds of samples involving StNP and/or SCF

3-3.4 Repulping

A quick repulping test shown in Figure 3-6 demonstrates the ability to maintain the tensile performance. There was no significant change in the performance when the hand sheets were prepared using normal pulp with the additives directly added or the additives previously incorporated within the sheet. This was important to demonstrate the feasibility of translating these formulated systems to industrial applications. The retention of the performance is supported by other studies as described by Hubbe et. al. [110]. Though, it is important to note that it is essential that the paper is never completely dried before attempting to repulp the hand sheet. Redispersing a completely dried hand sheet in water was challenging, (results not shown) and it took several days of mixing to produce a homogeneous slurry. This long mixing duration degraded the pulp fibers resulting in a hand sheet that was weaker than the control. Due to this factor, it is not possible to analyze results for repulping of a completely dried hand sheet.

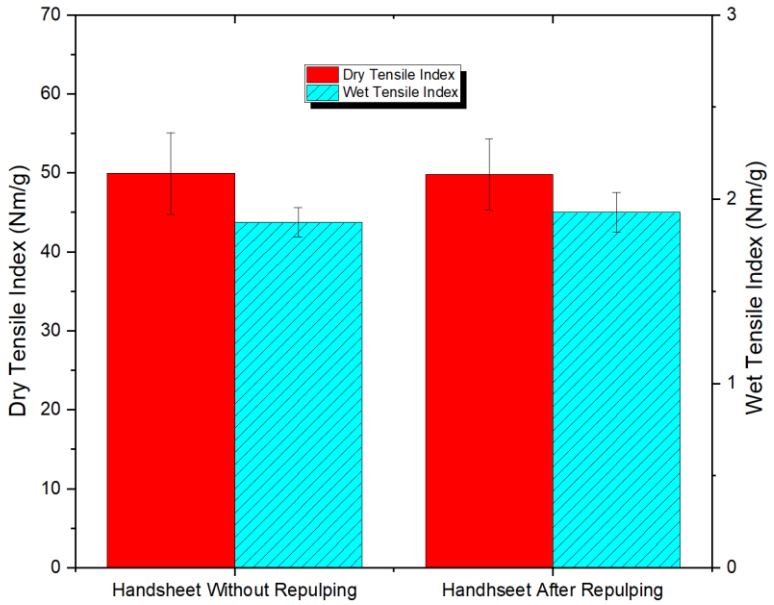

Figure 3- 6: Comparison of dry and wet tensile index of a hand sheet that had been repulped and one that had not been repulped.

3-4 Conclusions

The observations derived from this study confirmed the impact of the incorporation of StNPs in a HWp matrix. The addition of StNPs improved the dry tensile strength, but it reduced the wet tensile strength when compared to HWp controls. SCF and LCF were capable of improving both wet and dry tensile performance, but not when the components were used separately. The StNP:SCF system revealed that when 1 wt.% StNPs were used with SCF, the dry tensile index increased significantly. For the wet tensile index, having less than a StNP:SCF ratio of 3:2 was required to maintain the wet strength of the SCF without the negative effects of StNPs.

The filtration time of the hand sheets was not affected by the StNPs when used alone, but it displayed a negative effect when used with SCF. The filtration time increased by 8% for a 5 wt.% 1:1 StNP:SCF composition over a hand sheet with just 2.5% SCF.

It was demonstrated that there were no negative effects of repulping the hand sheets, and the dry and wet strength showed no significant difference between hand sheets before and after repulping.

Chapter 4: Antimicrobial Functionalized Starch Nanoparticles in Packaging Paper Formulation

4-1 Introduction

Starch is a natural, renewable polymer which has the capacity to fill the demand for affordable and sustainable polymers. It is largely used in industry as a filler or a template that requires further modification [111]. Starch can undergo a variety of chemical modifications, such as crosslinking, grafting, esterification, etherification, oxidation, and acidification [37], [112], [113]. Furthermore, starch is a biodegradable nanomaterial that can be used in agriculture [54], food [65], medicine [44], [45], [52], [68], and many others. Cationic starch nanoparticles (StNPs) were examined for their use as binding agents for cellulosic pulp material to enhance their tensile strength.

Smart packaging systems have generated increasing interest as a method to provide safe, high quality fresh foods to society. Currently, many food packaging systems use passive plastics to isolate the products from the external environment. Active packaging systems, on the other hand, actively change the environment in which the food products reside [13], [14]. Active packaging includes packages that have water or odour absorbing, antioxidizing, antimicrobial, or any combination of these properties [17], [26] within the packaging system. Direct antimicrobial systems use antimicrobial agents attached to the package or emitted in the packaging headspace. One of the most commonly used and highly studied antimicrobial agents is silver [30]. Recently, silver nanoparticles (AgNPs) have been gaining popularity as a newer form of silver that possesses unique properties with the potential of being a highly effective antimicrobial agent. Before these AgNP antimicrobial systems are commercially adopted, additional studies are necessary to ensure the safety, economic viability, and sustainability of the advanced packages [17], [25], [26].

Tannic acid (TA) possesses attractive characteristics for bio-based active packaging systems since it is biodegradable, biocompatible, and antibacterial [80]. These characteristics coupled with their capacity to reduce silver ions to form silver nanoparticles (AgNPs) [75], [77]–[79] offer interesting opportunities. The combination of StNPs, TA and AgNPs were examined in this study, particularly on their effectiveness as an active packaging system that maximizes sustainability.

4-2 Experimental

4-2.1 Materials

Cationic starch nanoparticles (StNPs) and hardwood pulp (HWp) are provided by EcoSynthetix Inc. (Burlington, ON, Canada). The StNPs are spherical in shape with an approximate diameter of 100-200 nm. Silver nitrate ($AgNO_3$) was purchased from ACROS. Potassium carbonate (K_2CO_3) was purchased from AMRESCO. Tannic acid ($C_{76}H_{52}O_{46}$) and Tris(hydroxymethyl)aminomethane ($NH_2C(CH_2OH)_3$) were purchased from Sigma-Aldrich. The bacteria used in this report are *Escherichia coli* (ATCC® PTA-4752™) and *Staphylococcus aureus* (ATCC® 6538™).

4-2.2 Additive Preparation

The concentrations of TA and $AgNO_3$ used are based on the protocol reported by Kim et al. [77] with procedural modifications.

4-2.2.1 TA Coated StNPs (TA@StNPs)

A 2.786 mg-TA/g-solution stock aqueous solution of TA was prepared by adding TA powder to deionized water and sonicated for approximately 30 minutes, or until it was completely dissolved. This solution was further diluted to achieve a final

concentration of either 25, 50, or 100 μM of TA. The volume of this solution was approximately 30 mL. To this, StNPs were added and dispersed with an ultrasonic probe, MICROSON model no. XL2000, at room temperature for approximately 10 minutes, or until no visible aggregation was evident. StNP concentrations of either 0.05, 0.1, or 0.2 wt.% were prepared. This mixture was adjusted to a pH of approximately 7 or higher using 0.125 M potassium carbonate. Finally, this mixture was divided into two separate sealed containers and kept for 24 hours at room temperature. The mixture turned from cloudy to a green-yellow colour, denoting the polymerization and coating of TA on StNPs. A total of 9 samples were prepared, covering all combinations of the three TA concentrations and three StNP concentrations.

4-2.2.2 Silver Nanoparticle Solution (AgNP/TA@StNPs)

A 0.946 mg-$AgNO_3$/g-solution stock solution of silver nitrate was prepared by adding silver nitrate crystals to deionized water, which quickly dissolved with gentle shaking. This stock solution was added to the TA@StNP mixture after 24 hours to achieve a final concentration of 250 μM $AgNO_3$. The mixture turned from green-brown to yellow-red, confirming the formation of AgNPs.

4-2.3 Hand Sheet Preparation

The hand sheet formation procedure is based on the TAPPI method T205 sp-02, with some minor modifications to adapt to available materials and equipment.

4-2.3.1 Stock Pulp Dispersion Preparation

A stock dispersion of pulp was prepared using the same method as mentioned in section 3-2.2.1 and is reworded here. First, 9.0 g of HWp was added to 291 mL of deionized water (3 wt.%) in a bowl with a SUNBEAM 2379-33A mixer attached. This

was mixed for 5 minutes on speed setting 3 while gently turning the bowl to ensure a homogeneous mixture. It was then diluted further by adding 300 mL of deionized water (1.5 wt.%) and mixed with a mechanical stirrer for 30 minutes such that there was a clear vortex. Finally, this was diluted again by adding 2.4 L of deionized water (0.3 wt.%) and mixed with a mechanical stirrer for an additional 1 hour. This dispersion was kept at room temperature in a sealed container. This stock dispersion settled quickly and must be mixed for at least 15 minutes prior to use.

4-2.3.2 Additive Pulp Dispersion

The additive mixture was prepared as described previously and diluted to 0.1 wt.% TA@StNPs. 475 mL of 0.3 wt.% stock pulp was mixed with a mechanical stirrer. To this, 75 mL of 0.1 wt.% solution was added dropwise to the dispersion and mixed for 30 minutes after the last drop was added. This dispersion yielded a hand sheet that contained 5% TA@StNP solid.

4-2.3.3 Hand Sheet Filtration and Drying

The filtration procedure follows the same method as described in section 3-2.2.3 and is reworded here. The filtration module contains a 200-mesh steel filter (75 μm pore size), with a 10 cm internal diameter, and a valve connected to vacuum. While the valve was closed, approximately 1 L of deionized water was added to the filtration setup. To this, 275 mL of the additive pulp dispersion (750 mg solids) was added. After 5 seconds, the vacuum valve was opened to commence the filtration process to prepare the hand sheet. The formed hand sheet was blotted dry with roughly 10 filter papers, WHATMAN 1 category no. 1001110 and 1001125. The dried hand sheet was then sandwiched between two dry filter papers., and pressed with a hydraulic press, MOTOMASTER

model no. 009-1096-8, at 50 psig for 5 minutes. The filter papers were replaced with new, dry filter papers and pressed again for an additional 2 minutes. This sandwich was then placed between two glass panes and placed in a drying oven for 24 hours at 80 °C. After 24 hours, the hand sheet was removed from the oven for further testing.

4-2.3.4 Dip Coating of Hand Sheets

A 25 mM or 50 mM solution of $AgNO_3$ was prepared in a container where the hand sheet sample may be completely immersed in the solution. Using tweezers, hand sheets that contained only TA@StNPs (100 μM TA, 0.2 wt.% StNP) were immersed in the solution for 1 minute. This was then blotted with approximately 5 filter papers, and then pressed for 2 minutes at 50 psig before drying in an oven between two glass panes. After 24 hours, the dipped hand sheet was removed for further testing.

4-2.3.5 Testing of Hand Sheets

Five different hand sheet samples were prepared according to the schematic shown in Figure 4-1. Hand sheets #2 - #5 were prepared using a 5 wt.% dry weight of additive. All TA@StNP solutions were prepared at concentrations of 100 μM and 0.2 wt.% for the TA and StNPs, respectively.

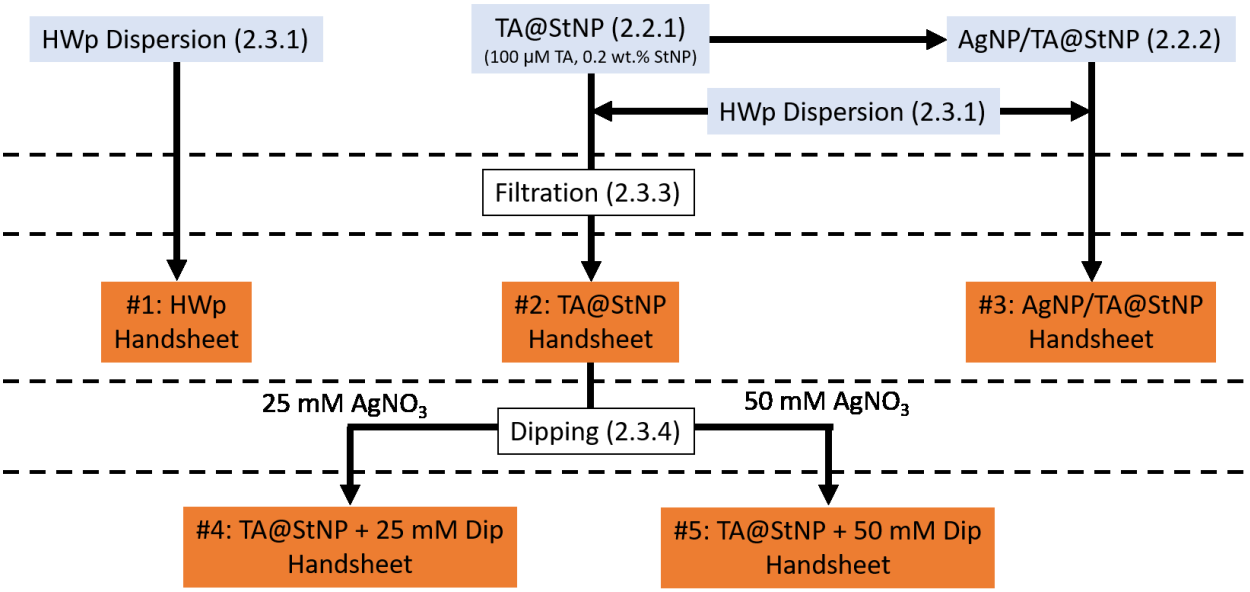

Figure 4- 1: Schematic of tested hand sheets.

4-2.4 Tensile Tests

The tensile tests follow the same procedure as outlined by section 3-2.3 and are reworded here. Tensile tests were performed on a CETR-UMT (BRUKER). To determine the tensile index of the samples as described in TAPPI method T494 om-01, the following procedure was followed. The hand sheets were cut into strips measuring 14 mm x 60 mm. These strips were inserted into the clamps with the distance between the clamps measuring 40 mm. The testing was performed at an elongation rate of 18 mm/min at room temperature. Wet tests were performed by depositing 30 µL of DI water on the strip, and once the droplet was completely absorbed the sample was loaded and tested. The calculation for tensile index is as follows:

$$TI\left(\frac{Nm}{gram}\right) = \frac{Tensile\ Strength\left(\frac{N}{m}\right)}{Grammage\left(\frac{grams}{m^2}\right)} = \frac{\left(\frac{F*g}{W}\right)}{\left(\frac{m}{L*W}\right)}$$

where F is the maximum force in kg as reported by the apparatus, g is gravitational acceleration constant, W is the width of the strip in meters (0.014 m), L is the length of the strip in meters (0.060 m), and m is the mass of the paper strip in grams.

4-2.5 Antibacterial Test

A suspension of *Escherichia coli* (*E. coli*) or *Staphylococcus aureus* (*S. aureus*) was cultured overnight at 37.5 °C in a shaking incubator, LAB-LINE model no. 4628. 6 mL of this culture was centrifuged and then resuspended in a 9 g/L saline solution (NaCl) to become a stock solution. A sample of this stock solution was used to determine the concentration by UV-Vis spectrophotometer, where an optical density at 600 nm (OD_{600}) of 0.2 was assumed to be 10^8 CFU/mL. Separately, the hand sheets were hole punched into small circular disks measuring 0.25 inches (6.35 mm) in diameter and weighing 2.5 ± 0.2 mg each. These disks were sterilized under ultraviolet light for 15 minutes before being tested. Ten of these disks were added to a 7 mL glass vial containing 4 mL of 4 x 10^8 CFU/mL of the specified bacterial culture. The vials were placed in the shaking incubator at 37.5 °C and tested at the 1.5, 3.0, 4.5, and 6.0 hour marks. At each specified time, the sample OD was measured by UV-Vis spectrophotometer at 550 nm for *E. coli* and 600 nm for *S. aureus* and the antibacterial activity units (U) was calculated as specified by Qiu et al. [61]:

$$U = \left(\frac{A_o - A}{A_o}\right)^{\frac{1}{2}}$$

where A is the OD of the specified sample and A_0 is the OD of the control.

4-2.6 Water Vapour Transmission Rate (WVTR)

The water vapour transmission rate (WVTR) was measured using the permeable cup method based on ASTM E96. A 125 mL mason jar containing 60 g of DI water was sealed with a regular mason jar screw band (5.65 cm diameter opening) and a hand sheet cut to fit a regular mason jar lid insert, such that the water vapour may only escape through the hand sheet. All samples were placed in a permeable container such that the samples were exposed to the lab atmosphere but were protected from excessive air flow. All five samples were concurrently tested in duplicate for a total of ten samples. The temperature within the container was 20.8 ± 0.3 °C and the relative humidity was 33 ± 3% for the duration of the test.

The WVTR was calculated as follows:

$$WVTR\ \left(\frac{g}{m^2 * hr}\right) = -\frac{1}{A} * \frac{dm_a}{dt} * \frac{m_h}{m_{avg}}$$

where dm_a/dt is the slope of the mass change of the entire apparatus over time with 5 measurements (including start mass) taken over the course of 48 hours. The exposed area, *A*, is the area of the mason jar screw band opening (which was 25.07 cm^2). m_h is the weight of the hand sheet cut to fit the mason jar lid insert and m_{avg} is the average weight of the cut hand sheets.

4-2.7 Characterizations

Transmission electron microscopy (TEM) was performed on a PHILIPS CM10. TEM was used to examine the size, morphology, and aggregation behaviour of the AgNPs. For hand sheet samples, the paper was shredded and dispersed in DI water before depositing on a copper grid for imaging.

Dynamic light scattering (DLS) was performed on MALVERN ZEN3690 DLS on diluted aqueous samples at 90° to determine the hydrodynamic radius (R_h) of the AgNPs and the TA@StNPs by examining the graphs in intensity mode and number mode.

Ultraviolet-visible (UV-vis) spectra was gathered on a VARIAN CARY 100 Bio spectrophotometer, and the tests were performed on diluted aqueous samples.

Thermogravimetric Analysis (TGA) was performed on a TGA Q500 V20.13 Build 39. TGA was run at 10.00 °C/min starting at 30 °C and ending at 700 °C. The purge flow was 100 mL/min of a nitrogen gas and air mixture in a 60:40 ratio.

4-3 Results and Discussion

4-3.1 AgNP/TA@StNP Size Characterization

The wavelength at peak absorbance (λ_{max}) measured on the UV-vis spectrophotometer is shown in Figure 4-2 for 9 samples of varying TA and StNP concentrations before and after the addition of $AgNO_3$. Before $AgNO_3$ was added, the peak absorbance showed minimal fluctuations with respect to TA or StNP concentration and was seen to be within a small range of 359 nm to 363 nm. However, 48 hours after the addition of $AgNO_3$, the peak absorbance increased to between 387 nm and 415 nm which corresponded to the typical range of AgNPs, as others have reported [114], [115]. This shift was associated to the local surface plasmonic resonance of the silver nanoparticles [116], confirming the formation of AgNPs. There was a slight inverse correlation between the λ_{max} and the concentration of both TA and StNPs in solution, with the lowest λ_{max} corresponding to the highest concentration of both TA and StNPs.

Additionally, Paramelle et al. [115] reported that the reduction in the size of AgNPs was correlated to the lowering of the λ_{max}. Thus, increasing the TA or StNP concentration will lead to a reduction in the size of AgNP.

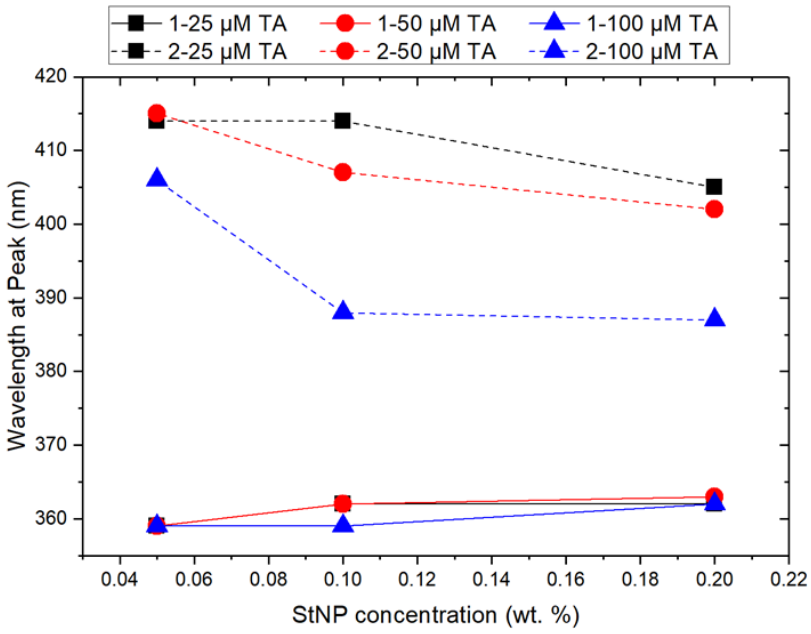

Figure 4- 2: Peak absorbance, λ_{max}, for aqueous AgNP/TA@StNPs with TA concentrations of 25 µM (black squares), 50 µM (red circles) and 100 µM (blue triangles). Measurements were taken before (solid lines) and after (dotted lines) the addition of $AgNO_3$

These results were confirmed and supported by DLS measurements shown in Figure 4-3. As two types of nanoparticles were present in solution, the size based on the number and intensity analysis could be used to isolate the mean size of the two particles without the need for physical separation. Intensity mode was biased toward larger particles; therefore, this would be representative of the TA@StNP size. Number mode was the opposite, and therefore represents the AgNP size. The results shown in Figure 4-3 indicated that the sizes of TA@StNPs were not correlated with the

concentration of either TA or StNP, whereas the size of AgNPs were correlated to the concentration of both TA and StNP. The lowest size of AgNPs was about 22 nm at the highest TA and StNP concentrations. The reasoning for the decrease in the size could be associated with the faster reaction rate, resulting in more nucleation of new AgNPs instead of growth on existing AgNPs [75], [79].

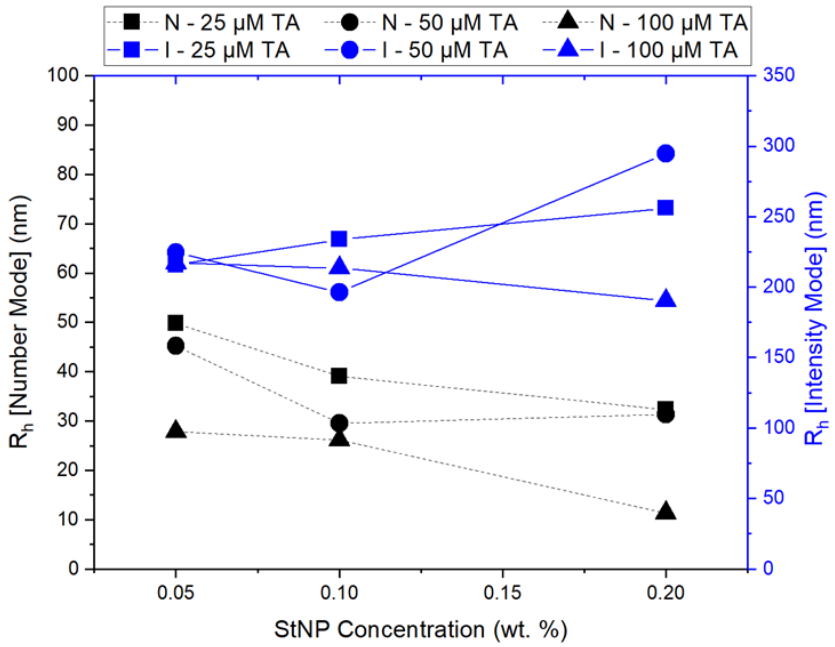

Figure 4- 3: DLS Measurements showing the hydrodynamic radius, R_h, of the particles in the AgNP/TA@StNP solution with TA concentrations of 25 µM (squares), 50 µM (circles) and 100 µM (triangles). The mean was calculated in intensity mode (blue solid lines) and number mode (black dotted lines)

A final confirmation of size was conducted using the TEM, where the sample with the highest concentration of both TA and StNPs possessed a diameter of approximately 20 nm, as shown in Figure 4-4. Many of the AgNPs found were in the bulk phase; however, Figure 4-4C shows clustered AgNPs immobilized on a structure with a diameter of approximately 600-700 nm. The intensity mode DLS data confirmed that

this structure was about the same size as a TA@StNP. Therefore, it is reasonable to assume that these clusters were TA@StNPs, where the AgNPs were likely to have chelated on its surface [79], [81]. Since the AgNPs were immobilized on the cationic TA@StNP surface, the electrostatic repulsion reduced aggregation.

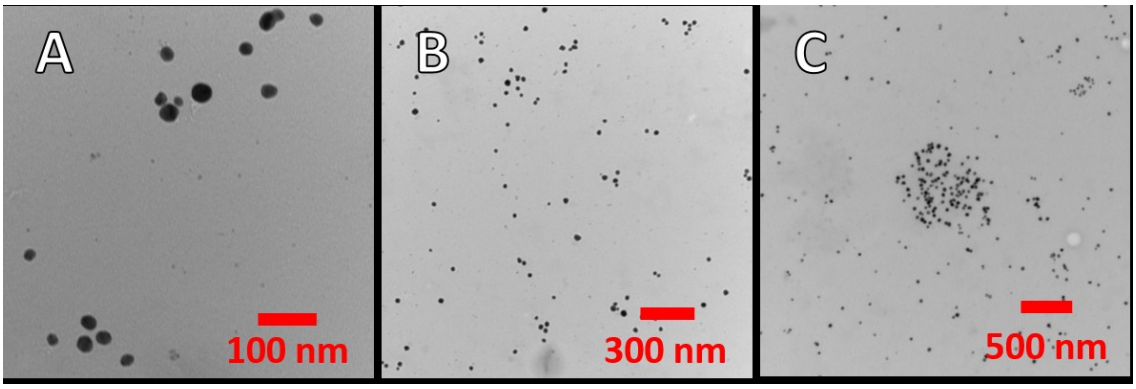

Figure 4- 4: TEM images of the AgNP/TA@StNP additive with 100 uM TA and 0.2 wt.% StNP shown at three different magnifications.

It was reported that a smaller AgNP size displays better antimicrobial efficacy [34], [117]. Therefore, for the hand sheets tested, filtration was only performed on the most optimal AgNPs; 100 µM TA and 0.2 wt.% StNPs.

4-3.2 AgNP Modified Hand Sheets

4-3.2.1 Tensile Performance

The tensile performance of the dry and wet tensile index of the modified hand sheets is shown in Figure 4-5. Without the addition of silver, the TA@StNP hand sheets displayed an increased tensile performance for both wet and dry strength, due to the interactions between the starch and pulp fibers. When silver was added before filtration (AgNP/TA@StNP), the dry performance was unaffected, but the wet performance was significantly enhanced. Samples dipped in 50 mM $AgNO_3$ possessed a significant

increase in the dry strength and a marginal increase in the wet strength. It is believed that the increased strength for the samples containing AgNP was associated with the reduction of porosity in the hand sheet and increased inter-fiber bonding [118].

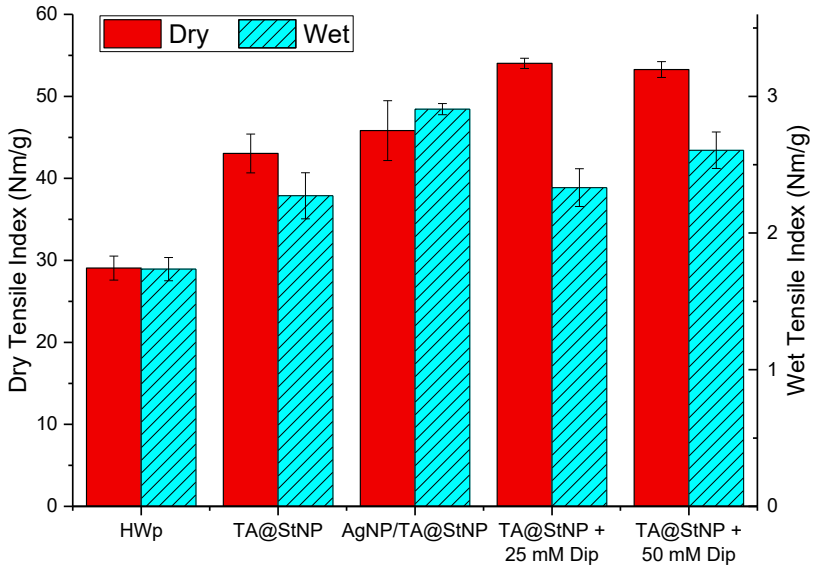

Figure 4- 5: Dry and wet tensile index of the tested hand sheets.

4-3.2.2 Water Vapour Transmission Rate (WVTR)

The water vapour transmission rate (WVTR) of the hand sheets is shown in Figure 4-6. While the transmission rate is important for packaging for moisture control, it can also indirectly provide information on the porosity of the hand sheets, as reported by Rhim et al. [119]. The range of permeability was similar to those reported in the review by Otoni et al. [25] for edible films. The values reported in that review were between 1 to 10 g mm m^{-2} h^{-1} kPa^{-1} or about 1.7 to 33.1 g m^{-2} h^{-1} after correction for the vapour pressure using Antoine's equation and assuming a hand sheet thickness of between 0.5 and 1 mm.

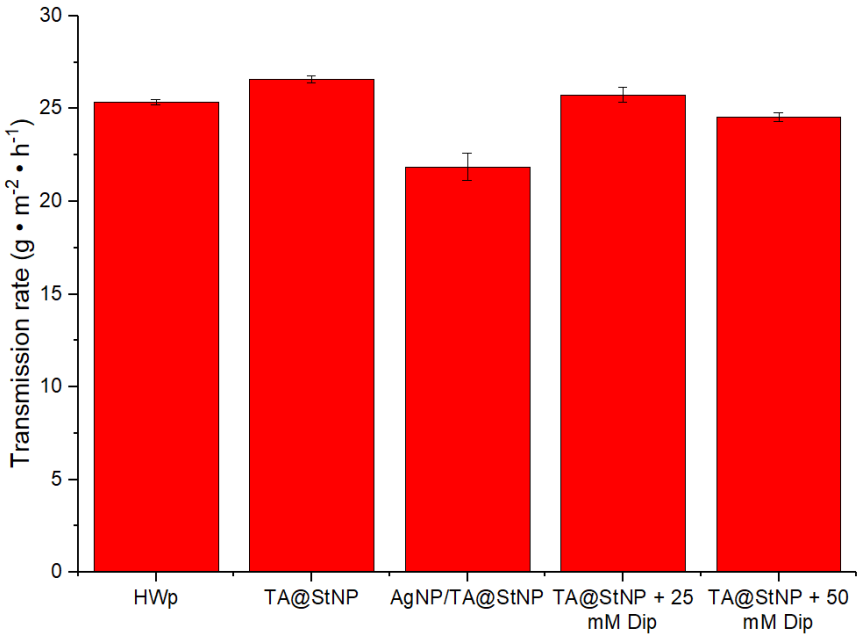

Figure 4- 6: Water vapour transmission rate (WVTR) of the tested hand sheets

The addition of TA@StNP yielded a WVTR of about 26.6 ± 0.2 g m^{-2} h^{-1}, which was 5% higher than the HWp control hand sheet with a WVTR of 25.4 ± 0.1 g m^{-2} h^{-1}. Hager et al. [120] suggested that for wheat gluten films, too much TA would increase the vapour permeation due an excess of free TA within the matrix that interfered with the homogeneity of the films. Additionally, using too much TA would increase the film's rigidity, causing small cracks that allow the vapour to permeate through. It is possible that the TA@StNP hand sheet was more rigid, causing a more porous structure, or that there was free tannic acid in the matrix, making it more susceptible for water vapour to permeate. However, these reasons were not apparent due to the relatively low concentration of TA present in the hand sheets (<1 wt.%).

WVTR decreased with the addition of AgNPs, when comparing the WVTR for TA@StNP, TA@StNP + 25 mM Dip, and TA@StNP + 50 mM Dip, the WVTR were 26.6 ± 0.2 g m^{-2} h^{-1}, 25.6 ± 0.4 g m^{-2} h^{-1}, and 24.6 ± 0.2 g m^{-2} h^{-1}, respectively. This decreasing trend was probably due to the AgNPs acting as fillers in the hand sheet matrix. This resulted in a more tortuous path for the water vapour to permeate or possibly an interaction with the water [121]–[126]. However, this reason alone was inadequate to explain the reduction in WVTR associated with the AgNP/TA@StNP hand sheet, with a value of 21.9 ± 0.71 g m^{-2} h^{-1} (-14% from HWp), which was significantly lower than all other hand sheets tested.

Additional factors that were associated with the reduced WVTR in the AgNP/TA@StNP hand sheet were the AgNP distribution and the TA crosslinking structure. The distribution of the AgNPs in the AgNP/TA@StNP hand sheet were contained within the bulk of the pulp matrix, causing a more tortuous path than the AgNPs concentrated at the surface. Furthermore, the TA in this hand sheet had reacted with silver ions before filtration, altering the way TA crosslinked to the pulp. This change counteracted the increased WVTR that was displayed by the TA@StNP hand sheet.

4-3.2.3 Antimicrobial Activity

The antimicrobial activity of the hand sheets was tested against gram-positive (*S. aureus*) and gram-negative (*E. coli*) bacteria and the results are shown in Figure 4-7. The results demonstrated that all the hand sheets with AgNPs possessed antibacterial characteristics when compared with the control hand sheet. Overall, the dipped hand sheets possessed the highest antibacterial activity, followed by AgNP/TA@StNP, and finally TA@StNP. While it is relatively well-known that TA possessed antimicrobial

properties [77], [80], [123], the addition of AgNPs further reinforced their capacity to eliminate bacteria [29], [117], [127]. However, the antibacterial activity of AgNP/TA@StNP was similar to TA alone. The reason could be due to factors surrounding the AgNP concentration, distribution, and morphology.

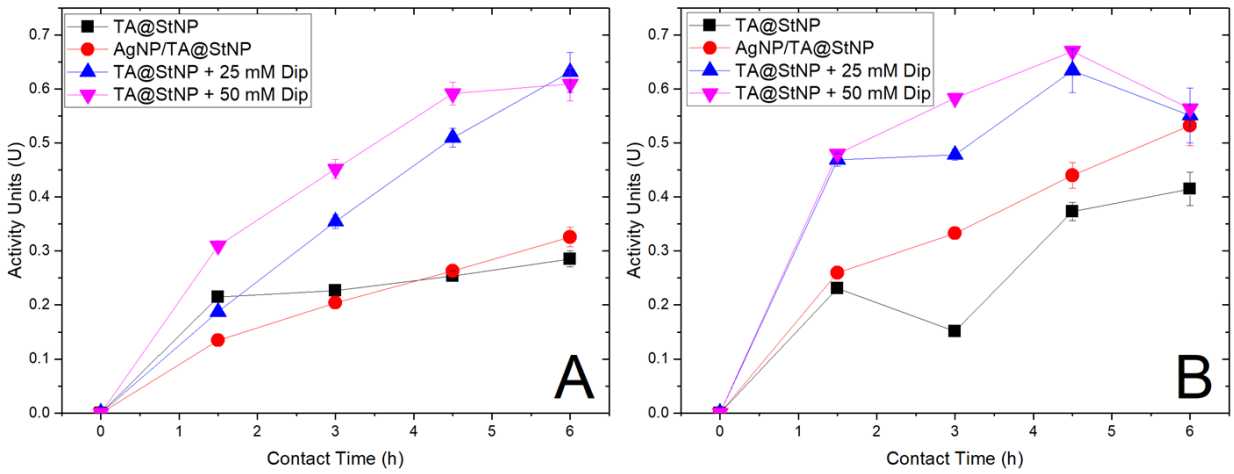

Figure 4- 7: Antibacterial activity units (U) of the tested hand sheets at over time (h) against *E. coli* (A) and *S. aureus* (B).

TEM images of the AgNPs in the dipped hand sheet were measured and they are shown in Figure 4-8. The nanoparticles from the dipping technique possessed a larger and more irregular shape compared to the small spherical particles that were shown previously in Figure 4-4. The irregularly shaped nanoparticles could have been beneficial for antimicrobial efficacy [128], [129] or they may have had no effect at all [130] when compared to spherical AgNPs. Conversely, smaller particles are known to have better antimicrobial properties [34], [117], thus the morphology of the AgNPs was insufficient to explain the difference in results for the two methods.

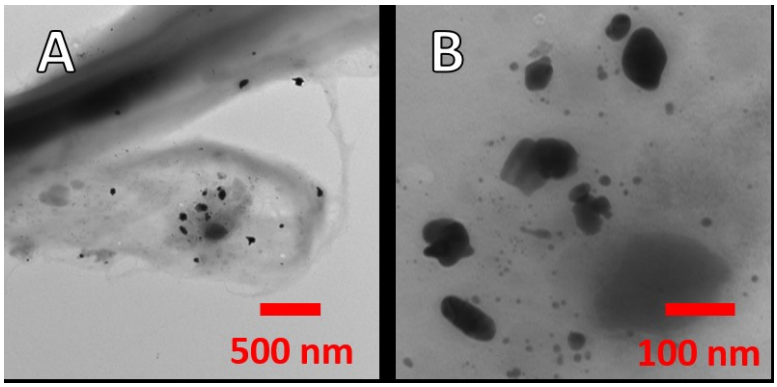

Figure 4- 8: TEM images of a shredded TA@StNP + 50 mM Dip hand sheet shown at two (A, B) different magnifications.

A more probable reason for the improved performance of dipped hand sheets was that the AgNPs were located on the surface of the hand sheet. Thus, the AgNPs were more accessible for interactions with the bacteria compared to the AgNP/TA@StNP sheet. This was further exacerbated by the higher wet tensile strength and lower permeability of the AgNP/TA@StNP hand sheet; both these conditions reduced the amounts of exposed AgNPs. A third factor would be related to the total amount of silver present on the hand sheet. However, this quantity had not been directly determined, but it was inferred from the TGA data shown in Figure 4-9.

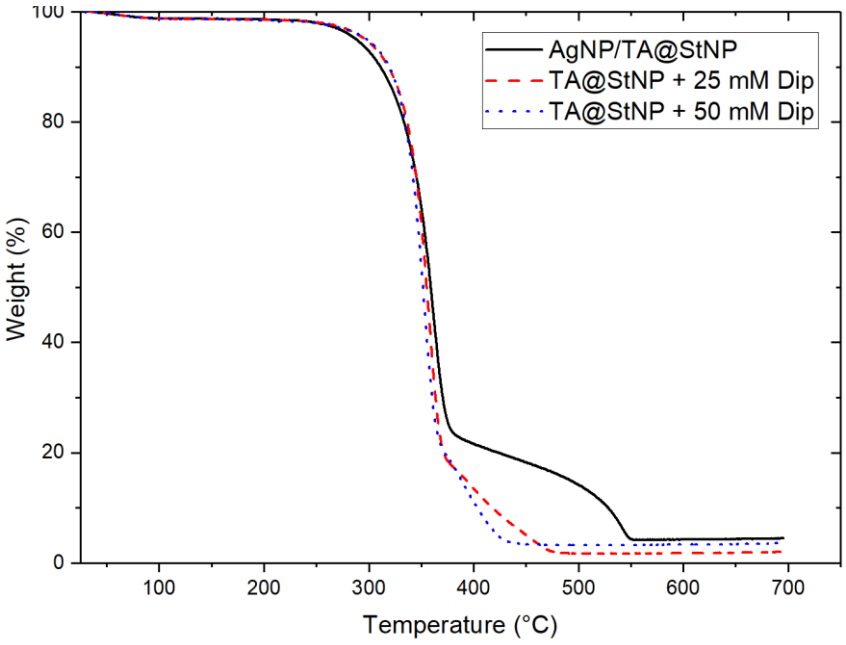

Figure 4- 9: TGA data showing the mass loss of the hand sheets containing AgNPs

From the TGA data, the majority of mass loss was between 300-375 °C, which is associated to the pyrolysis of the pulp [131]. A noted difference of the three curves was within the last 20% of decomposition between 375-550 °C. This could be associated to the degradation of TA in the presence of oxygen as reported by Xia et al. [132]. However, TA constitutes less than 1 wt.% of the hand sheet, meaning that the unoxidized TA must form a protective layer on the pulp. The two dipped hand sheets confirmed that a quicker degradation occurred when the TA had been reacted with more silver ions resulting in a positive correlation between the amount of unoxidized TA and the time required for the protective layer to decompose. Therefore, the AgNP/TA@StNP hand sheet possessed the most unreacted TA, then the TA@StNP + 25 mM Dip hand sheet and lastly, the TA@StNP + 50 mM Dip hand sheet. Since the total quantity of TA

on each hand sheet was identical, the total mass of AgNPs was directly related to the amount of reacted TA.

The two dipped hand sheets displayed similar antibacterial properties and the TGA data confirmed that they also possessed similar amounts of AgNPs. Likewise, the TGA data showed less AgNP formation on the AgNP/TA@StNP hand sheet, and consequently, reduced antibacterial properties. Out of the three factors discussed, the concentration, or total amount of silver on the hand sheet was deemed to be the main contributor to the antimicrobial activity of the hand sheets.

4-4 Conclusions

AgNPs were synthesized with TA@StNP as the reducing and stabilizing agents. The AgNPs were mostly spherical and their size could be tuned between 22 to 100 nm. The smallest size was produced in a 100 μM TA and 0.2 wt.% StNPs. AgNP modified pulp hand sheets were prepared using two approaches. In the first method, the 22 nm spherical AgNPs were incorporated within the bulk of the pulp matrix, and the hand sheet achieved the highest wet tensile index of ~3 Nm/g, and the lowest water vapour permeability of 21.9 g m^{-2} h^{-1}. In the second method, TA@StNP hand sheets were dipped in $AgNO_3$ solution, and irregular 100 nm AgNPs were reduced on the surface of the hand sheet, yielding a much higher content of AgNP. This system displayed the best antimicrobial activity, and the highest dry tensile index of ~53 Nm/g.

Chapter 5: Sizing effect of Water Dispersible Amphiphilic Starch Nanoparticles in Paper Products

5-1 Introduction

The purpose of paper sizing is to prevent the permeation of liquids into the paper, and sizing agents, such as alkenyl succinic anhydride (ASA) and alkyl ketene dimer (AKD) are commonly used. Though these sizing agents are widely used for paper making, rapid hydrolysis in aqueous environments remains a challenge. In order to reduce the hydrolyzing effects, stabilizers, such as cationic starches are being used. [86]–[88].

Paper packaging can be seen as an alternative to unsustainable oil-based plastic packaging [38]. Unfortunately, paper displays a lower tensile strength than plastics, especially when wet, which reduces its potential as a suitable packaging material. Paper sizing is an effective way to increase the paper's overall mechanical strength because it prolongs the time the paper stays dry, which negates the need for wet strength in paper.

Starch nanoparticles are renewable and biocompatible materials, making them ideal additives for dry strength enhancement and paper sizing in alternative packaging materials. Starch is one of the most common paper additives for reasons, such as improving paper strength, printability, and surface sizing [103], [133]. Starch nanoparticles take advantage of these properties of macroscopic starch, and the increased surface area and reduced viscosity make it an attractive additive [36].

Amphiphilic bio-based nanoparticles have been reported in literature [95], [96], but the use of dried powders in the wet-end for paper sizing has rarely been reported. These ready to use powders allow for the rapid preparation of additives that reduce the complexity of the paper manufacturing processes.

5-2 Experimental

5-2.1 Materials

Hydrophobic cationic starch nanoparticles (StNPs) and hardwood pulp (HWp) are provided by EcoSynthetix Inc. (Burlington, ON, Canada). The StNPs are spherical in shape with an approximate diameter of 100-200 nm.

5-2.2 Hand Sheet Preparation

The hand sheet formation procedure is based on the TAPPI method T205 sp-02, but it was modified to accommodate the available materials and equipment.

5-2.2.1 Stock Pulp Dispersion Preparation

The stock pulp dispersion was prepared in the same method as described in section 3-2.2.1 and is reworded here. A bulk dispersion of HWp was prepared by adding 9.0 g of pulp to 291 mL of deionized water (3 wt.% solids). This was mixed using a stand mixer, SUNBEAM 2379-33A, on speed setting 3 in a small mixing bowl. The bowl was gently turned to ensure homogeneous mixing for 5 minutes. To this, 300 mL of deionized water was added (1.5 wt.% solids) and mixed on a mechanical stirrer for 30 minutes with a sufficient vortex. This was then diluted with 2.4 L of deionized water (0.3 wt.% solids) and placed under the mechanical stirrer for an additional hour at approximately the same RPM. After which, the pulp dispersion was lidded for storage at room temperature until needed. This mixture must be redispersed for approximately 15 minutes before and during usage as the pulp will settle very quickly.

5-2.2.2 Additive Pulp Dispersion

The additive dispersion was prepared with the same method as mentioned in 3-2.2.2 and is reworded here. The hydrophobic starch was dispersed in DI water using an ultrasonic probe, MICROSON model no. XL2000, at room temperature. A 0.1 wt.% concentration of StNP was prepared. The additive dispersion was added dropwise to the stock pulp dispersion to prepare formulations with 1, 3, 5, or 8 wt.% additive by solids.

5-2.2.3 Hand Sheet Filtration and Drying

The filtration was performed with the same procedure as mentioned in section 3-2.2.3 and reworded here. Filtration was performed with a 200-mesh steel filter (75 μm pore size) to create 10 cm diameter hand sheets. First, approximately 1 L of deionized water was added to the filtration setup which rested on top of the mesh due to surface tension. To that, the additive pulp dispersion was added such that there were 750 mg of solids. After approximately 5 seconds a mild vacuum was applied to the bottom of the filtration setup to pull the water through leaving a wet hand sheet. This was then blotted dry with approximately 9 filter papers, WHATMAN 1 category no. 1001110 and 1001125. Then, each hand sheet was pressed with a hydraulic press, MOTOMASTER model no. 009-1096-8, for 5 minutes at 50 psig while sandwiched between two dry filter papers, and then for an additional 2 minutes with two new dry filter papers. Finally, the sheet was put in the oven at 80 °C for 24 hours between two glass panes to prevent curling and wrinkles from forming. After the 24 hours the sheet was removed and could be further tested.

5-2.3 Tensile Test

The tensile tests were performed using the same procedure as mentioned in section 3-2.3 and reworded here. Tensile tests were completed with a CETR-UMT (BRUKER). As a guide to determine tensile index a procedure was adapted from the TAPPI method T494 om-01. The hand sheets were cut into rectangles measuring 6 cm x 1.4 cm. The distance between the clamps when the sample was loaded was 4 cm. The test was run at an elongation rate of 18 mm/min at room temperature. To perform the wet tensile test 30 µL of DI water was deposited in the center of the paper strip. Once the droplet was completely absorbed, the strip was loaded into the clamps to test.

The tensile index was calculated with the following equation:

$$TI\left(\frac{Nm}{gram}\right) = \frac{Tensile\ Strength\left(\frac{N}{m}\right)}{Grammage\left(\frac{grams}{m^2}\right)} = \frac{\left(\frac{F * g}{W}\right)}{\left(\frac{m}{L * W}\right)}$$

where F is the maximum force in kg as reported by the apparatus, g is gravitational acceleration constant, W is the width of the strip in meters (0.014 m), L is the length of the strip in meters (0.060 m), and m is the mass of the paper strip in grams.

5-2.4 Hand Sheet Drying Rate

The drying rate of the hand sheets was tested to see if the hydrophobic additive had any influence on the drying time of the hand sheets. A quick test was performed on a balance with an infrared heater attachment, and it was set to 105 °C for the duration of the drying test. The hand sheets were prepared using the normal filtration procedure, but they were not dried completely. This wet hand sheet was transferred to the heated

balance and measurements were conducted every 30 seconds until a constant weight was achieved.

5-2.5 Characterization

Dynamic contact angle was performed on a FIBRO mo. DAT 1100. To test the hydrophobicity of the sample and the absorption time, dynamic contact angle measurements were determined. Each sample was tested with a minimum of 10 droplets, and each droplet comprised of 4 µL of DI water.

Surface tension measurements were performed on a DATAPHYSICS mo. DCAT 11. This test was used to determine the surface activity of the StNPs and the saturation concentration of the hydrophobic starch NP.

5-3 Results and Discussion

5-3.1 Surface Tension Measurements

The surface tension measurements shown in Figure 5-1 indicated that the StNPs possessed a surfactant like behaviour in water. A reduction in the surface tension of the water to about 42 mN/m at a saturation of about 15 g/L. A similar result was reported by Chen Li et al. for acid hydrolyzed starch nanocrystals with the surface tension reduced to 45 mN/m at concentration of 30 g/L [134]. However, it is important to note that these concentrations are significantly higher than concentrations used in the additive solution, which was at about 1 g/L (0.1 wt.%). Thus, the saturation point would never be reached when the paper slurry was being formed during the wet-end of production. Additionally, the solution became noticeably turbid at 0.1 wt.% suggesting the aggregation of StNPs.

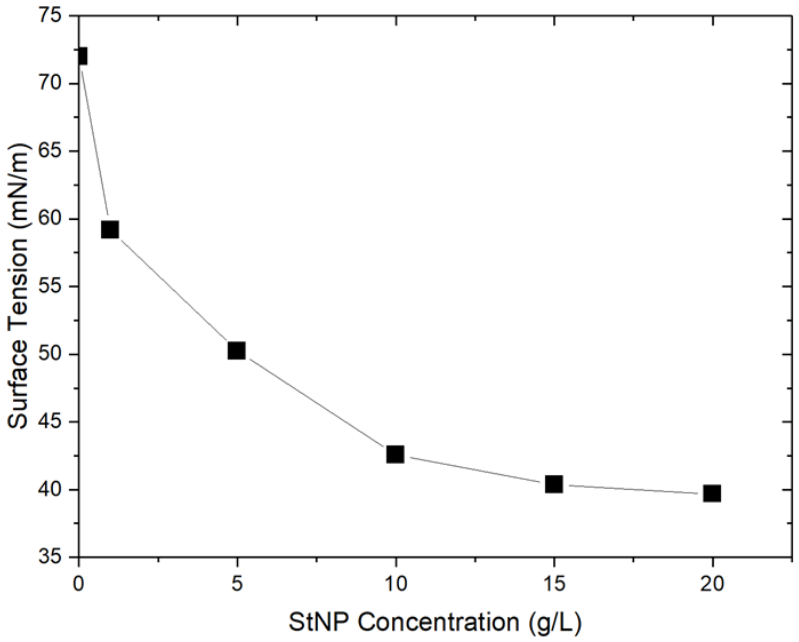

Figure 5- 1: Surface tension measurements of water at different concentrations of StNPs

5-3.2 Tensile Strength

The tensile strength shown in Figure 5-2 indicate that the dry tensile index of the hand sheets increased with the addition of hydrophobic starch, however the wet tensile strength decreased marginally. The dry strength could be attributed to the electrostatic binding of StNPs to the pulp matrix that promote the intermolecular interactions between the pulp fibres in the hand sheet. The dry strength increased sharply by 11.7 Nm/g (+30%) over the control with just 1 wt.% hydrophobic StNPs and approached a maximum of 28.3 Nm/g (+72%) more than the control at 5 wt.% StNPs.

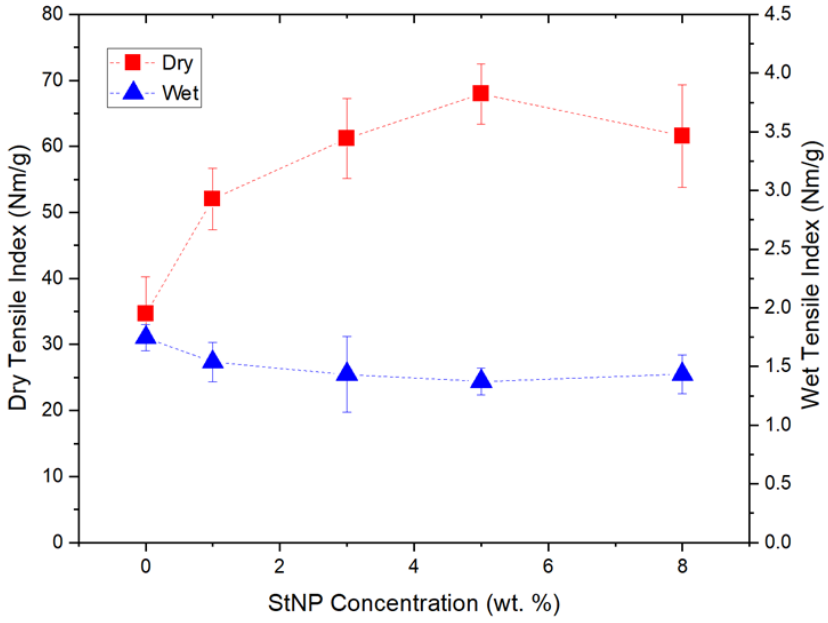

Figure 5- 2: Dry and wet tensile index of hand sheets with varying dry weight of StNPs

The reduction in the wet strength was likely due to the testing methods. The wet test could only be performed when the water droplet was completely absorbed, while at the same time the absorption was delayed due to the hydrophobic StNPs. Thus, the tensile strip was exposed to water for longer than a minute, which might cause premature failure of the strips. This also causes a detachment of the starch from the pulp matrix, reducing its ability to hold the fibers together. It would be ideal to assume that given these factors, the StNPs had very little effect on the wet strength. It was also apparent that the dry and wet strength moved towards that of the control when greater than 5 wt.% StNP was used. This trend could be associated with aggregation of StNPs in the pulp matrix at the higher additive level.

5-3.3 Contact Angle

Figures 5-3 and 5-4 show the dynamic contact angle of the hand sheets with different amounts of StNPs. As the proportion of StNPs increased to 3 to 5 wt.%. the water contact angle of the hand sheets increased and then decreased beyond 5 wt.%. The 5 wt.% hand sheets had the highest recorded contact angle at 0.1 s, which was 93° ± 5°. At 8 wt.% this decreased to 80° ± 5° due to the potential aggregation. Figure 5-3B also displays the hand sheets resistance to wetting, with the maximum time between droplet deposition and absorption being about 3 s. The mechanisms of this resistance trend are still under investigation.

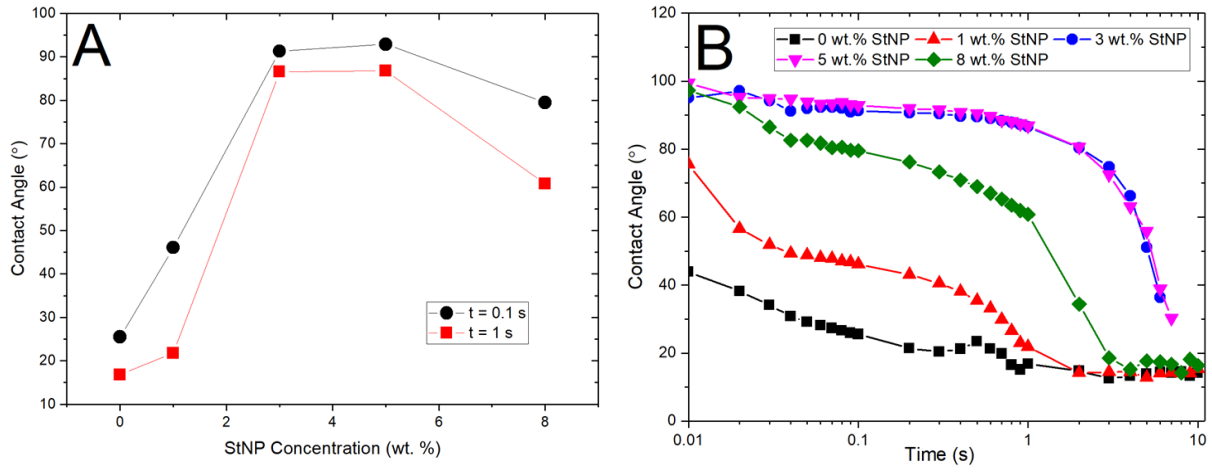

Figure 5- 3: The relationship between contact angle and (A) StNP concentration at varying times or (B) time at varying StNP concentrations

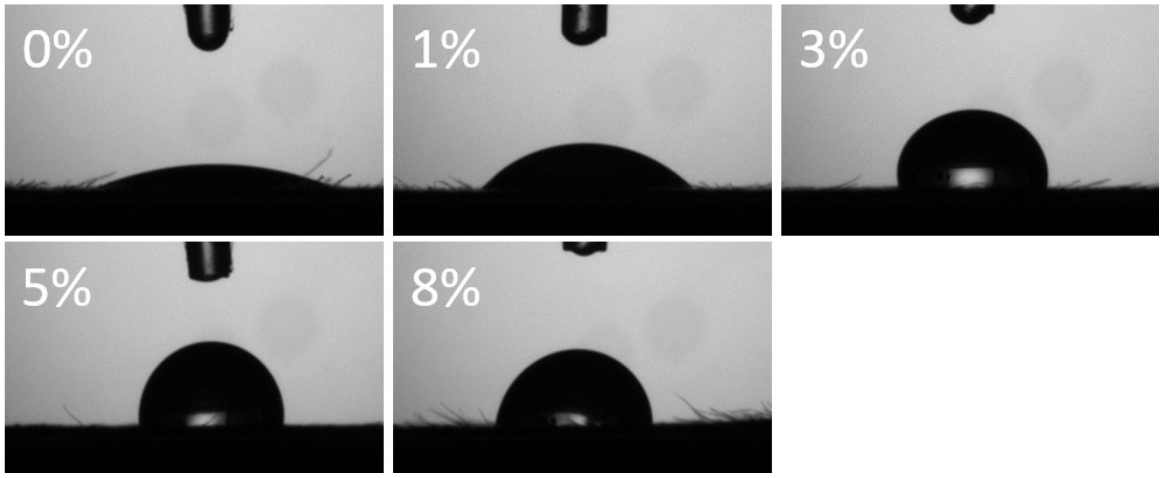

Figure 5- 4: Pictures of droplets during contact angle measurements at varying amounts of StNPs. All images were taken at 0.1 seconds with a 4 µL droplet of water.

5-3.4 Drying Rate

Figure 5-5 shows the drying rate of the hand sheets containing 0, 1, and 8 wt.% StNPs. The curves of all three samples exhibited the same profile. Therefore, the rate of drying under these conditions did not depend on the amount of StNPs present in the hand sheet. It can be assumed that the hand sheets prepared using these StNPs will dry at the same rate.

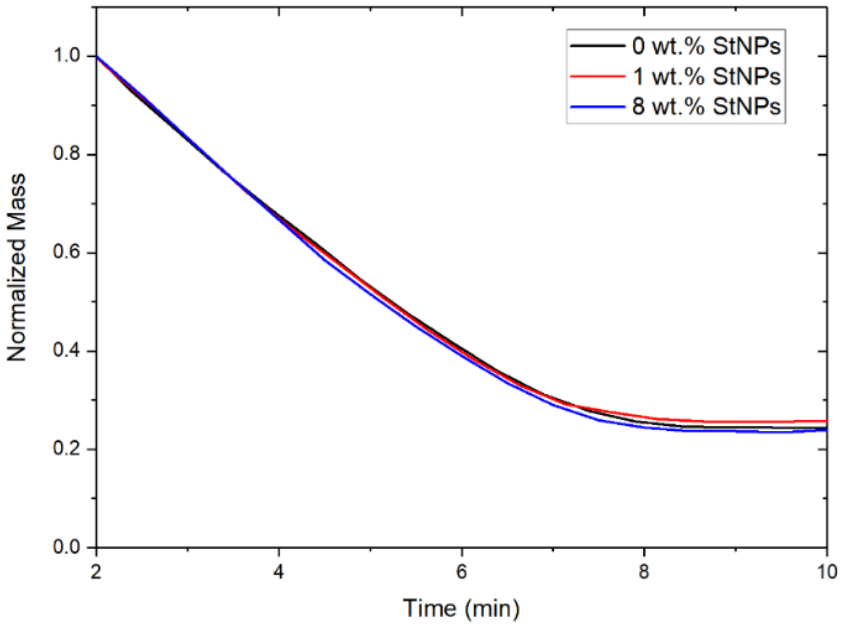

Figure 5- 5: Change in normalized mass over time to demonstrate the drying rate of hand sheets

5-4 Conclusions

Hydrophobically modified StNPs could be used to prepare hydrophobic hand sheets. These hand sheets had the additional benefit of increasing dry tensile strength over pulp paper with a maximum increase of 72% over the control at 5 wt.% StNPs. However, the wet tensile strength displayed a slight decrease.

The hydrophobic properties of the hand sheets were confirmed by the contact angle exceeded 90° when measured at 0.1 s and at StNP level as low as 3 wt.%. However, the contact angle decreased significantly when StNP content exceeded 5 wt.%. The hydrophobic properties of the hand sheet had no noticeable effect on the drying rate, which was a promising result for an industrial paper mill.

Chapter 6: Conclusions, Future Work, and Recommendations

6-1: Conclusions for the Work Presented in Chapter 3

Hand sheets containing a mixture of cationic StNPs and cellulose fibers exhibited great promise for improving the tensile properties of pulp-paper. Cationic StNPs could be used as a wet and dry strengthening agent when used in combination with SCF. The optimal composition was using at least 1 wt.% StNPs to significantly improve the dry strength of the hand sheets at all compositions of StNPs and SCF. The optimal wet strength composition occurs when hand sheets contain less than a 3:2 ratio of StNP:SCF. Moreover, the hand sheets maintain these favourable properties after repulping, and this protocol will be tested in a pilot process in Brazil.

Additionally, the StNPs had a minimal impact on the filtration time during the preparation of the hand sheets. However, interaction of StNPs and SCF increased the filtration time compared to when SCFs were used with no StNPs.

6-2: Conclusions for the Work Presented in Chapter 4

Pulp paper prepared with AgNPs possessed antimicrobial characteristics suitable for active packaging solutions in food applications. To reduce the amount of food waste worldwide, active packaging solutions will reduce microbial growth and extend the shelf-life of foods to make them safer. Silver ions were reduced by TA coated StNPs to form AgNPs, and their size could be tuned by the concentrations of TA or StNPs. The smallest size of AgNPs could be achieved with the highest concentrations of TA and StNPs, and the largest sizes at the lowest concentrations of TA and StNPs. Hand sheets were prepared with AgNPs by either the wet-end or dry-end addition process. Both methods yielded hand sheets that displayed antimicrobial activity against *E. coli*

and *S. aureus*. The dry-end addition of AgNPs possessed a higher activity which was associated to a higher concentration of silver in the hand sheet. The hand sheets containing AgNPs displayed improved tensile strength and lowered water vapour permeability. These additional features were associated with the reduced porosity that resulted to an increase in the inter-fiber bonding.

6-3: Conclusions for the Work Presented in Chapter 5

Industrial paper sizing requires freshly prepared ingredients in order to maintain the sizing efficiency. However, the water dispersible amphiphilic StNPs showed great potential as a ready-to-use product for paper sizing. The pulp paper could be given hydrophobic characteristics with contact angles greater than 90° with the addition of 3 to 5 wt.% of hydrophobic StNPs. These papers could resist wetting for several seconds, and afterwards the water diffused into the pulp network. The hand sheets had additional benefits of increased dry tensile strength and similar drying profile as normal hand sheets.

6-4: Future Work and Recommendations for Work Presented in Chapter 3

The StNP:SCF system shows promise in improving the wet and dry strength of paper. Further studies would focus on determining its potentials and limitations. Additional mechanical properties, such as tearing strength or burst strength should be determined. Additionally, barrier properties, like gas permeabilities are key factors that should be considered when designing packaging materials. As such, these tests are to ensure that they meet the criteria for the packaged goods.

6-5: Future Work and Recommendations for Work Presented in Chapter 4

This study demonstrates the possibilities of using AgNP for active packaging systems. The amount of silver on the hand sheets should be quantified, where the distribution of AgNPs in the hand sheet should be established. Potentiometric titration to determine the leaching of silver ions from the paper should be determined.

The silver content should be optimized to minimize the amount of necessary silver. The dipped hand sheets can be prepared in various concentrations of $AgNO_3$ solutions and the AgNP/TA@StNP hand sheet could be prepared to contain higher amounts of AgNP.

Finally, additional properties, such as contact angle, oxygen permeability, and oxygen scavenging would provide valuable insight for their use in packaging applications.

6-6: Future Work and Recommendations for Work Presented in Chapter 5

It is highly recommended that the mechanism describing the behaviour of amphiphilic StNPs greater than 5 wt.% should be elucidated. This is critical for improving the hydrophobic properties and wet strength of the hand sheets. StNPs with various levels of modification should be examined.

Understanding the mechanisms for the delay in the water absorption for the hydrophobic hand sheet will offer new opportunities to design various types of

hydrophobic papers. The migration and orientation of the StNPs during filtration, drying, and wetting should be studied in more detail.

References

[1] J. R. Jambeck *et al.*, “Plastic waste inputs from land into the ocean,” *Am. Assoc. Adv. Sci.*, vol. 347, no. 6223, pp. 768–771, 2015.

[2] Y. Belhouari *et al.*, “Together for our Ocean. International Coastal Clean Up 2017 Report,” 2017.

[3] C. M. Boerger, G. L. Lattin, S. L. Moore, and C. J. Moore, “Plastic ingestion by planktivorous fishes in the North Pacific Central Gyre,” *Mar. Pollut. Bull.*, vol. 60, no. 12, pp. 2275–2278, 2010.

[4] J. Li, H. Liu, and J. Paul Chen, “Microplastics in freshwater systems: A review on occurrence, environmental effects, and methods for microplastics detection,” *Water Res.*, vol. 137, pp. 362–374, 2018.

[5] “What We Know About: Plastic Marine Debris,” *NOAA Marine Debris*, no. September. 2011.

[6] M. B. Phillips and T. H. Bonner, “Occurrence and amount of microplastic ingested by fishes in watersheds of the Gulf of Mexico,” *Mar. Pollut. Bull.*, vol. 100, no. 1, pp. 264–269, 2015.

[7] K. Jabeen *et al.*, “Microplastics and mesoplastics in fish from coastal and fresh waters of China,” *Environ. Pollut.*, vol. 221, pp. 141–149, 2017.

[8] R. Yamashita, H. Takada, M. aki Fukuwaka, and Y. Watanuki, “Physical and chemical effects of ingested plastic debris on short-tailed shearwaters, Puffinus tenuirostris, in the North Pacific Ocean,” *Mar. Pollut. Bull.*, vol. 62, no. 12, pp. 2845–2849, 2011.

[9] D. de A. Miranda and G. F. de Carvalho-Souza, “Are we eating plastic-ingesting fish?,” *Mar. Pollut. Bull.*, vol. 103, no. 1–2, pp. 109–114, 2016.

[10] H. Friege, “Sustainable Chemistry – A concept with important links to waste management,” *Sustain. Chem. Pharm.*, vol. 6, no. May, pp. 57–60, 2017.

[11] M. V. Gooch and A. Felfel, “$27 Billion Revisited the Cost of Canada’s Annual Food Waste,” pp. 1–41, 2014.

[12] CEC, *Characterization and Management of Food Loss and Waste in North America*, no. June. 2017.

[13] V. A. Jideani and K. Vogt, “Antimicrobial Packaging for Extending the Shelf Life of Bread—A Review,” *Crit. Rev. Food Sci. Nutr.*, vol. 56, no. 8, pp. 1313–1324, 2016.

[14] P. Appendini and J. H. Hotchkiss, “Review of antimicrobial food packaging,” *Innovative Food Science and Emerging Technologies*, vol. 3, no. 2. pp. 113–126,

2002.

[15] M. L. Rooney, “Introduction to active food packaging technologies,” in *Innovations in Food Packaging*, J. H. Han, Ed. San Diego: Elsevier, 2005, pp. 63–77.

[16] J. P. Kerry, M. N. O’Grady, and S. A. Hogan, “Past, current and potential utilisation of active and intelligent packaging systems for meat and muscle-based products: A review,” *Meat Sci.*, 2006.

[17] I. Ahmed *et al.*, “A comprehensive review on the application of active packaging technologies to muscle foods,” *Food Control*, vol. 82, pp. 163–178, 2017.

[18] B. Malhotra, A. Keshwani, and H. Kharkwal, “Antimicrobial food packaging: Potential and pitfalls,” *Frontiers in Microbiology*. 2015.

[19] S. D. F. Mihindukulasuriya and L. T. Lim, “Nanotechnology development in food packaging: A review,” *Trends Food Sci. Technol.*, vol. 40, pp. 149–167, 2014.

[20] P. J. P. Espitia, W. X. Du, R. de J. Avena-Bustillos, N. de F. F. Soares, and T. H. McHugh, “Edible films from pectin: Physical-mechanical and antimicrobial properties - A review,” *Food Hydrocoll.*, vol. 35, pp. 287–296, 2014.

[21] P. J. P. Espitia, N. de F. F. Soares, J. S. dos R. Coimbra, N. J. de Andrade, R. S. Cruz, and E. A. A. Medeiros, “Zinc Oxide Nanoparticles: Synthesis, Antimicrobial Activity and Food Packaging Applications,” *Food Bioprocess Technol.*, vol. 5, no. 5, pp. 1447–1464, 2012.

[22] C. Sharma, R. Dhiman, N. Rokana, and H. Panwar, “Nanotechnology : An Untapped Resource for Food Packaging,” vol. 8, no. September, 2017.

[23] I. R. Ariyarathna, R. M. P. I. Rajakaruna, and D. N. Karunaratne, “The rise of inorganic nanomaterial implementation in food applications,” *Food Control*, vol. 77, pp. 251–259, 2017.

[24] J. Gomez-Estaca, C. Lopez-de-Dicastillo, P. Hernandez-Munoz, R. Catala, and R. Gavara, “Advances in antioxidant active food packaging,” *Trends Food Sci. Technol.*, vol. 35, no. 1, pp. 42–51, 2014.

[25] C. G. Otoni *et al.*, “Recent Advances on Edible Films Based on Fruits and Vegetables-A Review,” *Compr. Rev. Food Sci. Food Saf.*, vol. 16, pp. 1151–1169, 2017.

[26] Z. Fang, Y. Zhao, R. D. Warner, and S. K. Johnson, “Active and intelligent packaging in meat industry,” *Trends Food Sci. Technol.*, vol. 61, no. 2, pp. 60–71, 2017.

[27] C. G. Otoni, P. J. P. Espitia, R. J. Avena-Bustillos, and T. H. McHugh, “Trends in antimicrobial food packaging systems: Emitting sachets and absorbent pads,” *Food Research International*. 2016.

[28] M. J. Hajipour *et al.*, “Antibacterial properties of nanoparticles,” *Trends in Biotechnology*. 2012.

[29] S. M. Dizaj, F. Lotfipour, M. Barzegar-Jalali, M. H. Zarrintan, and K. Adibkia, “Antimicrobial activity of the metals and metal oxide nanoparticles,” *Mater. Sci. Eng. C*, vol. 44, pp. 278–284, 2014.

[30] O. Choi, K. K. Deng, N.-J. J. Kim, L. Ross, R. Y. Surampalli, and Z. Hu, “The inhibitory effects of silver nanoparticles, silver ions, and silver chloride colloids on microbial growth,” *Water Res.*, vol. 42, no. 12, pp. 3066–3074, 2008.

[31] Y.-K. Jo, B. H. Kim, and G. Jung, “Antifungal Activity of Silver Ions and Nanoparticles on Phytopathogenic Fungi,” *Plant Dis.*, vol. 93, no. 10, pp. 1037–1043, 2009.

[32] C. N. Lok *et al.*, “Proteomic analysis of the mode of antibacterial action of silver nanoparticles,” *J. Proteome Res.*, vol. 5, no. 4, pp. 916–924, 2006.

[33] Z. M. Xiu, Q. B. Zhang, H. L. Puppala, V. L. Colvin, and P. J. J. Alvarez, “Negligible particle-specific antibacterial activity of silver nanoparticles,” *Nano Lett.*, vol. 12, no. 8, pp. 4271–4275, 2012.

[34] A. Ivask *et al.*, “Toxicity mechanisms in Escherichia coli vary for silver nanoparticles and differ from ionic silver,” *ACS Nano*, vol. 8, no. 1, pp. 374–386, 2014.

[35] L. Wei, J. Lu, H. Xu, A. Patel, Z. S. Chen, and G. Chen, “Silver nanoparticles: Synthesis, properties, and therapeutic applications,” *Drug Discov. Today*, vol. 20, no. 5, pp. 595–601, 2015.

[36] D. Le Corre and H. Angellier-Coussy, “Preparation and application of starch nanoparticles for nanocomposites: A review,” *React. Funct. Polym.*, vol. 85, pp. 97–120, 2014.

[37] N. Masina *et al.*, “A review of the chemical modification techniques of starch,” *Carbohydr. Polym.*, vol. 157, pp. 1226–1236, 2017.

[38] F. Xie, E. Pollet, P. J. Halley, and L. Avérous, “Starch-based nano-biocomposites,” *Prog. Polym. Sci.*, vol. 38, no. 10–11, pp. 1590–1628, 2013.

[39] E. Šárka and V. Dvořáček, “Waxy starch as a perspective raw material (a review),” *Food Hydrocoll.*, vol. 69, pp. 402–409, 2017.

[40] X. Li, Y. Qin, C. Liu, S. Jiang, L. Xiong, and Q. Sun, “Size-controlled starch nanoparticles prepared by self-assembly with different green surfactant: The effect of electrostatic repulsion or steric hindrance,” *Food Chem.*, vol. 199, pp. 356–363, 2016.

[41] D. Liu, Q. Wu, H. Chen, and P. R. Chang, “Transitional properties of starch colloid with particle size reduction from micro- to nanometer,” *J. Colloid Interface Sci.*,

vol. 339, no. 1, pp. 117–124, 2009.

[42] D. Song, Y. S. Thio, and Y. Deng, “Starch nanoparticle formation via reactive extrusion and related mechanism study,” *Carbohydr. Polym.*, vol. 85, no. 1, pp. 208–214, 2011.

[43] S. B. Haaj, W. Thielemans, A. Magnin, and S. Boufi, “Starch nanocrystal stabilized pickering emulsion polymerization for nanocomposites with improved performance,” *ACS Appl. Mater. Interfaces*, vol. 6, no. 11, pp. 8263–8273, 2014.

[44] E. Masoudipour, S. Kashanian, A. H. Azandaryani, K. Omidfar, and E. Bazyar, “Surfactant effects on the particle size, zeta potential, and stability of starch nanoparticles and their use in a pH-responsive manner,” *Cellulose*, vol. 24, no. 10, pp. 4217–4234, 2017.

[45] F. Ye, M. Miao, B. Jiang, O. H. Campanella, Z. Jin, and T. Zhang, “Elucidation of stabilizing oil-in-water Pickering emulsion with different modified maize starch-based nanoparticles,” *Food Chem.*, vol. 229, pp. 152–158, 2017.

[46] J. Safari, P. Aftabi, M. Ahmadzadeh, M. Sadeghi, and Z. Zarnegar, “Sulfonated starch nanoparticles: An effective, heterogeneous and bio-based catalyst for synthesis of 14-aryl-14-H-dibenzo[a,j]xanthenes,” *J. Mol. Struct.*, vol. 1142, pp. 33–39, 2017.

[47] H. Angellier, L. Choisnard, S. Molina-Boisseau, P. Ozil, and A. Dufresne, “Optimization of the preparation of aqueous suspensions of waxy maize starch nanocrystals using a response surface methodology,” *Biomacromolecules*, vol. 5, no. 4, pp. 1545–1551, 2004.

[48] J. P. Robin, C. Mercier, R. Charbonniere, and a Guilbot, “Lintnerized Starches. Gel Filtration and Enzymatic Studies of Insoluble Residues from Prolonged Acid Treatment of Potato Starch,” *Cereal Chem.*, vol. 51. pp. 389–405, 1974.

[49] A. Shaabani, A. Rahmati, and Z. Badri, “Sulfonated cellulose and starch: New biodegradable and renewable solid acid catalysts for efficient synthesis of quinolines,” *Catal. Commun.*, vol. 9, no. 1, pp. 13–16, 2008.

[50] M. A. El-Sheikh, “New technique in starch nanoparticles synthesis,” *Carbohydr. Polym.*, vol. 176, pp. 214–219, 2017.

[51] Y. Qin, C. Liu, S. Jiang, L. Xiong, and Q. Sun, “Characterization of starch nanoparticles prepared by nanoprecipitation: Influence of amylose content and starch type,” *Ind. Crops Prod.*, vol. 87, pp. 182–190, 2016.

[52] S. Ge *et al.*, “Characterizations of Pickering emulsions stabilized by starch nanoparticles: Influence of starch variety and particle size,” *Food Chem.*, vol. 234, pp. 339–347, 2017.

[53] A. Hebeish, M. H. El-Rafie, M. A. EL-Sheikh, and M. E. El-Naggar, “Ultra-Fine Characteristics of Starch Nanoparticles Prepared Using Native Starch With and

Without Surfactant," *J. Inorg. Organomet. Polym. Mater.*, vol. 24, no. 3, pp. 515–524, 2014.

[54] M. Bayat Tork, R. Khalilzadeh, and H. Kouchakzadeh, "Efficient harvesting of marine Chlorella vulgaris microalgae utilizing cationic starch nanoparticles by response surface methodology," *Bioresour. Technol.*, vol. 243, pp. 583–588, 2017.

[55] Y. Ding and J. Kan, "Optimization and characterization of high pressure homogenization produced chemically modified starch nanoparticles," *J. Food Sci. Technol.*, vol. 54, no. 13, pp. 4501–4509, 2017.

[56] X. Wang, J. Cheng, G. Ji, X. Peng, and Z. Luo, "Starch nanoparticles prepared in a two ionic liquid based microemulsion system and their drug loading and release properties," *RSC Adv.*, vol. 6, no. 6, pp. 4751–4757, 2016.

[57] L. Qi, G. Ji, Z. Luo, Z. Xiao, and Q. Yang, "Characterization and Drug Delivery Properties of OSA Starch-Based Nanoparticles Prepared in [C 3 OHmim]Ac-in-Oil Microemulsions System," *ACS Sustain. Chem. Eng.*, vol. 5, no. 10, pp. 9517–9526, 2017.

[58] D. Dehghan Baniani, R. Bagheri, and A. Solouk, "Preparation and characterization of a composite biomaterial including starch micro/nano particles loaded chitosan gel," *Carbohydr. Polym.*, vol. 174, pp. 633–645, 2017.

[59] Y. Ding, J. Zheng, X. Xia, T. Ren, and J. Kan, "Preparation and characterization of resistant starch type IV nanoparticles through ultrasonication and miniemulsion cross-linking," *Carbohydr. Polym.*, vol. 141, pp. 151–159, 2016.

[60] Y. Huang *et al.*, "Ultra-small and innocuous cationic starch nanospheres: Preparation, characterization and drug delivery study," *Int. J. Biol. Macromol.*, vol. 58, pp. 231–239, 2013.

[61] C. Qiu *et al.*, "Preparation and characterization of essential oil-loaded starch nanoparticles formed by short glucan chains," *Food Chem.*, vol. 221, pp. 1426–1433, 2017.

[62] X. Li *et al.*, "Synthesis and study the properties of StNPs/gum nanoparticles for salvianolic acid B-oral delivery system," *Food Chem.*, vol. 229, pp. 111–119, 2017.

[63] Q. Liu *et al.*, "Enhanced dispersion stability and heavy metal ion adsorption capability of oxidized starch nanoparticles," *Food Chem.*, vol. 242, no. March 2017, pp. 256–263, 2018.

[64] C. Liu, Y. Qin, X. Li, Q. Sun, L. Xiong, and Z. Liu, "Preparation and characterization of starch nanoparticles via self-assembly at moderate temperature," *Int. J. Biol. Macromol.*, vol. 84, pp. 354–360, 2016.

[65] X. Li, N. Ji, M. Li, S. Zhang, L. Xiong, and Q. Sun, "Morphology and Structural

Properties of Novel Short Linear Glucan/Protein Hybrid Nanoparticles and Their Influence on the Rheological Properties of Starch Gel," *J. Agric. Food Chem.*, vol. 65, no. 36, pp. 7955–7965, 2017.

[66] Q. Sun, G. Li, L. Dai, N. Ji, and L. Xiong, "Green preparation and characterisation of waxy maize starch nanoparticles through enzymolysis and recrystallisation," *Food Chem.*, vol. 162, pp. 223–228, 2014.

[67] J. Yang *et al.*, "Fabrication and characterization of hollow starch nanoparticles by gelation process for drug delivery application," *Carbohydr. Polym.*, vol. 173, pp. 223–232, 2017.

[68] C. Liu, M. Li, N. Ji, J. Liu, L. Xiong, and Q. Sun, "Morphology and Characteristics of Starch Nanoparticles Self-Assembled via a Rapid Ultrasonication Method for Peppermint Oil Encapsulation," *J. Agric. Food Chem.*, vol. 65, no. 38, pp. 8363–8373, 2017.

[69] L. Li *et al.*, "Fabrication of self-assembled folate–biotin-quaternized starch nanoparticles as co-carrier of doxorubicin and siRNA," *J. Biomater. Appl.*, vol. 32, no. 5, pp. 587–597, 2017.

[70] L. Dai, C. Li, J. Zhang, and F. Cheng, "Preparation and characterization of starch nanocrystals combining ball milling with acid hydrolysis," *Carbohydr. Polym.*, vol. 180, no. September 2017, pp. 122–127, 2018.

[71] Y. Shi *et al.*, "Room temperature preparation of fluorescent starch nanoparticles from starch-dopamine conjugates and their biological applications," *Mater. Sci. Eng. C*, vol. 82, no. September 2017, pp. 204–209, 2018.

[72] A. S. Abreu *et al.*, "Antimicrobial nanostructured starch based films for packaging," *Carbohydr. Polym.*, vol. 129, pp. 127–134, 2015.

[73] P. Samyn, A. Barhoum, T. Öhlund, and A. Dufresne, "Review: nanoparticles and nanostructured materials in papermaking," *J. Mater. Sci.*, pp. 146–184, 2017.

[74] E. Schmidt *et al.*, "Chemical composition, olfactory evaluation and antioxidant effects of essential oil from Mentha x piperita.," *Nat. Prod. Commun.*, vol. 4, no. 8, pp. 1107–12, Aug. 2009.

[75] Y. Cao, R. Zheng, X. Ji, H. Liu, R. Xie, and W. Yang, "Syntheses and characterization of nearly monodispersed, size-tunable silver nanoparticles over a wide size range of 7-200 nm by tannic acid reduction," *Langmuir*, vol. 30, no. 13, pp. 3876–3882, 2014.

[76] Y. Fang *et al.*, "Universal one-pot, one-step synthesis of core–shell nanocomposites with self-assembled tannic acid shell and their antibacterial and catalytic activities," *J. Appl. Polym. Sci.*, vol. 135, no. 6, pp. 4–11, 2018.

[77] T. Y. Kim, S. H. Cha, S. Cho, and Y. Park, "Tannic acid-mediated green synthesis of antibacterial silver nanoparticles," *Arch. Pharm. Res.*, vol. 39, no. 4, pp. 465–

473, 2016.

[78] K. Ranoszek-Soliwoda *et al.*, “The role of tannic acid and sodium citrate in the synthesis of silver nanoparticles,” *J. Nanoparticle Res.*, vol. 19, no. 8, 2017.

[79] Z. Yi *et al.*, “Green, effective chemical route for the synthesis of silver nanoplates in tannic acid aqueous solution,” *Colloids Surfaces A Physicochem. Eng. Asp.*, vol. 392, no. 1, pp. 131–136, 2011.

[80] N. Sahiner, S. Sagbas, M. Sahiner, C. Silan, N. Aktas, and M. Turk, “Biocompatible and biodegradable poly(Tannic Acid) hydrogel with antimicrobial and antioxidant properties,” *Int. J. Biol. Macromol.*, vol. 82, pp. 150–159, 2016.

[81] Z. Shi *et al.*, “Enhanced colloidal stability and antibacterial performance of silver nanoparticles/cellulose nanocrystal hybrids,” *J. Mater. Chem. B*, vol. 3, no. 4, pp. 603–611, 2015.

[82] L. Pan, H. Wang, C. Wu, C. Liao, and L. Li, “Tannic-Acid-Coated Polypropylene Membrane as a Separator for Lithium-Ion Batteries,” *ACS Appl. Mater. Interfaces*, vol. 7, no. 29, pp. 16003–16010, 2015.

[83] S. Hong, Y. S. Na, S. Choi, I. T. Song, W. Y. Kim, and H. Lee, “Non-Covalent Self-Assembly and Covalent Polymerization Co-Contribute to Polydopamine Formation,” pp. 4711–4717, 2012.

[84] Y. Fang, J. Tan, H. Choi, S. Lim, and D. H. Kim, “Highly sensitive naked eye detection of Iron (III) and H2O2using poly-(tannic acid) (PTA) coated Au nanocomposite,” *Sensors Actuators, B Chem.*, vol. 259, pp. 155–161, 2018.

[85] A. Lepetit, R. Drolet, B. Tolnai, D. Montplaisir, R. Lucas, and R. Zerrouki, “Microfibrillated cellulose with sizing for reinforcing composites with LDPE,” *Cellulose*, vol. 24, no. 10, pp. 4303–4312, 2017.

[86] A. Kumar, N. K. Bhardwaj, and S. P. Singh, “Sizing performance of alkenyl succinic anhydride (ASA) emulsion stabilized by polyvinylamine macromolecules,” *Colloids Surfaces A Physicochem. Eng. Asp.*, vol. 539, no. September 2017, pp. 132–139, 2018.

[87] B. Sun, Q. Hou, Z. Liu, Z. He, and Y. Ni, “Stability and efficiency improvement of ASA in internal sizing of cellulosic paper by using cationically modified cellulose nanocrystals,” *Cellulose*, vol. 21, no. 4, pp. 2879–2887, 2014.

[88] C. Dang, M. Xu, Y. Yin, and J. Pu, “Preparation and characterization of hydrophobic non-crystal microporous starch (NCMS) and its application in food wrapper paper as a sizing agent,” *BioResources*, vol. 12, no. 3, pp. 5775–5789, 2017.

[89] H. Winkler, W. Vorwerg, and R. Rihm, “Thermal and mechanical properties of fatty acid starch esters,” *Carbohydr. Polym.*, vol. 102, no. 1, pp. 941–949, 2014.

[90] D. Muscat, R. Adhikari, S. McKnight, Q. Guo, and B. Adhikari, “The physicochemical characteristics and hydrophobicity of high amylose starch-glycerol films in the presence of three natural waxes,” *J. Food Eng.*, vol. 119, no. 2, pp. 205–219, 2013.

[91] S. Acosta, A. Jiménez, M. Cháfer, C. González-Martínez, and A. Chiralt, “Physical properties and stability of starch-gelatin based films as affected by the addition of esters of fatty acids,” *Food Hydrocoll.*, vol. 49, pp. 135–143, 2015.

[92] J. Yuan, T. Wang, X. Huang, and W. Wei, “Effect of Wet-End Additives on the Results of Alkyl Ketene Dimer Sizing after Adding Bacterial Cellulose,” vol. 11, no. 4, pp. 9280–9289, 2016.

[93] V. Guazzotti, S. Limbo, L. Piergiovanni, R. Fengler, D. Fiedler, and L. Gruber, “A study into the potential barrier properties against mineral oils of starch-based coatings on paperboard for food packaging,” *Food Packag. Shelf Life*, vol. 3, pp. 9–18, 2015.

[94] E. Calce, E. Mignogna, V. Bugatti, M. Galdiero, V. Vittoria, and S. De Luca, “Pectin functionalized with natural fatty acids as antimicrobial agent,” *Int. J. Biol. Macromol.*, vol. 68, pp. 28–32, 2014.

[95] A. Cova, A. J. Sandoval, V. Balsamo, and A. J. Müller, “The effect of hydrophobic modifications on the adsorption isotherms of cassava starch,” *Carbohydr. Polym.*, vol. 81, no. 3, pp. 660–667, 2010.

[96] B. Wei, B. Sun, B. Zhang, J. Long, L. Chen, and Y. Tian, “Synthesis, characterization and hydrophobicity of silylated starch nanocrystal,” *Carbohydr. Polym.*, vol. 136, pp. 1203–1208, 2016.

[97] T. De Assis, L. W. Reisinger, L. Pal, J. Pawlak, H. Jameel, and R. W. Gonzalez, “Understanding the Effect of Machine Technology and Cellulosic Fibers on Tissue Properties – A Review,” *BioResources*, vol. 13, no. 2, pp. 1–37, 2018.

[98] C. J. Biermann, *Handbook of Pulping and Papermaking*, 2nd ed. Corvallis, Oregon: Elsevier, 1996.

[99] S. Boufi, I. González, M. Delgado-Aguilar, Q. Tarrès, and P. Mutjé, “Nanofibrillated cellulose as an additive in papermaking process,” *Cellul. Nanofibre Compos. Prod. Prop. Appl.*, vol. 154, pp. 153–173, 2017.

[100] J. Shen, P. Fatehi, and Y. Ni, “Biopolymers for surface engineering of paper-based products,” *Cellulose*, vol. 21, no. 5, pp. 3145–3160, 2014.

[101] S. K. Gulsoy and S. Erenturk, “Improving strength properties of recycled and virgin pulp mixtures with dry strength agents,” *Starch/Staerke*, vol. 69, no. 3–4, pp. 1–8, 2017.

[102] M. Wu, W. LV, F. Wang, Z. Long, J. Chen, and C. Dong, “Preparation of dialdehyde chitosan/crosslinked amino starch and its effect on paper strength,”

Cellul. Chem. Technol., vol. 52, pp. 43–49, 2018.

[103] M. Ulbrich, S. Radosta, B. Kießler, and W. Vorwerg, “Interaction of cationic starch derivatives and cellulose fibres in the wet end and its correlation to paper strength with a statistical evaluation,” *Starch/Staerke*, vol. 64, no. 12, pp. 972–983, 2012.

[104] S. H. Osong, S. Norgren, and P. Engstrand, “Processing of wood-based microfibrillated cellulose and nanofibrillated cellulose, and applications relating to papermaking: a review,” *Cellulose*, vol. 23, no. 1, pp. 93–123, 2016.

[105] F. W. Brodin, Ø. W. Gregersen, and K. Syverud, “Cellulose nanofibrils: Challenges and possibilities as a paper additive or coating material - A review,” *Nord. Pulp Pap. Res. J.*, vol. 29, no. 1, pp. 156–166, 2014.

[106] Y. Hamzeh, S. Sabbaghi, A. Ashori, A. Abdulkhani, and F. Soltani, “Improving wet and dry strength properties of recycled old corrugated carton (OCC) pulp using various polymers,” *Carbohydr. Polym.*, vol. 94, no. 1, pp. 577–583, 2013.

[107] S. K. Gulsoy, “Effects of cationic starch addition and pulp beating on strength properties of softwood kraft pulp,” *Starch/Staerke*, vol. 66, no. 7–8, pp. 655–659, 2014.

[108] A. Ghasemian, M. Ghaffari, and A. Ashori, “Strength-enhancing effect of cationic starch on mixed recycled and virgin pulps,” *Carbohydr. Polym.*, vol. 87, no. 2, pp. 1269–1274, 2012.

[109] M. Lund and C. Felby, “Wet strength improvement of unbleached kraft pulp through laccase catalyzed oxidation,” *Enzyme Microb. Technol.*, vol. 28, no. 9–10, pp. 760–765, 2001.

[110] M. A. Hubbe, R. A. Venditti, and O. J. Rojas, “What happens to cellulosic fibers during papermaking and recycling? A review,” *BioResources*, vol. 2, no. 4, pp. 739–788, 2007.

[111] A. Gandini, T. M. Lacerda, A. J. F. Carvalho, and E. Trovatti, “Progress of Polymers from Renewable Resources: Furans, Vegetable Oils, and Polysaccharides,” *Chem. Rev.*, vol. 116, no. 3, pp. 1637–1669, 2016.

[112] Q. Chen *et al.*, “Recent progress in chemical modification of starch and its applications,” *RSC Adv.*, vol. 5, no. 83, pp. 67459–67474, 2015.

[113] R. N. Tharanathan, “Starch - Value addition by modification,” *Crit. Rev. Food Sci. Nutr.*, vol. 45, no. 5, pp. 371–384, 2005.

[114] Z. Li, M. Zhang, D. Cheng, and R. Yang, “Preparation of silver nano-particles immobilized onto chitin nano-crystals and their application to cellulose paper for imparting antimicrobial activity,” *Carbohydr. Polym.*, vol. 151, pp. 834–840, 2016.

[115] D. Paramelle, A. Sadovoy, S. Gorelik, P. Free, J. Hobley, and D. G. Fernig, “A rapid method to estimate the concentration of citrate capped silver nanoparticles

from UV-visible light spectra," *Analyst*, vol. 139, no. 19, pp. 4855–4861, 2014.

[116] S. Linic, P. Christopher, H. Xin, and A. Marimuthu, "Catalytic and photocatalytic transformations on metal nanoparticles with targeted geometric and plasmonic properties," *Acc. Chem. Res.*, vol. 46, no. 8, pp. 1890–1899, 2013.

[117] N. Durán, M. Durán, M. B. de Jesus, A. B. Seabra, W. J. Fávaro, and G. Nakazato, "Silver nanoparticles: A new view on mechanistic aspects on antimicrobial activity," *Nanomedicine Nanotechnology, Biol. Med.*, vol. 12, no. 3, pp. 789–799, 2016.

[118] T. Tabarsa, S. Sheykhnazari, A. Ashori, M. Mashkour, and A. Khazaeian, "Preparation and characterization of reinforced papers using nano bacterial cellulose," *Int. J. Biol. Macromol.*, vol. 101, pp. 334–340, 2017.

[119] J. W. Rhim, L. F. Wang, Y. Lee, and S. I. Hong, "Preparation and characterization of bio-nanocomposite films of agar and silver nanoparticles: Laser ablation method," *Carbohydr. Polym.*, vol. 103, no. 1, pp. 456–465, 2014.

[120] A. S. Hager, K. J. R. Vallons, and E. K. Arendt, "Influence of gallic acid and tannic acid on the mechanical and barrier properties of wheat gluten films," *J. Agric. Food Chem.*, vol. 60, no. 24, pp. 6157–6163, 2012.

[121] D. Le Corre, J. Bras, and A. Dufresne, "Starch Nanoparticles : A Review," *Biomacromolecules*, vol. 11, pp. 1139–1153, 2010.

[122] F. Chivrac, H. Angellier-Coussy, V. Guillard, E. Pollet, and L. Avérous, "How does water diffuse in starch/montmorillonite nano-biocomposite materials?," *Carbohydr. Polym.*, vol. 82, no. 1, pp. 128–135, Aug. 2010.

[123] A. Jiménez, M. J. Fabra, P. Talens, and A. Chiralt, "Edible and Biodegradable Starch Films: A Review," *Food Bioprocess Technol.*, vol. 5, no. 6, pp. 2058–2076, 2012.

[124] B. Kuswandi, "Environmental friendly food nano-packaging," *Environ. Chem. Lett.*, vol. 15, no. 2, pp. 205–221, 2017.

[125] J. Y. Huang, X. Li, and W. Zhou, "Safety assessment of nanocomposite for food packaging application," *Trends Food Sci. Technol.*, vol. 45, no. 2, pp. 187–199, 2015.

[126] F. Ortega, L. Giannuzzi, V. B. Arce, and M. A. García, "Active composite starch films containing green synthetized silver nanoparticles," *Food Hydrocoll.*, vol. 70, pp. 152–162, 2017.

[127] J. A. Lemire, J. J. Harrison, and R. J. Turner, "Antimicrobial activity of metals: mechanisms, molecular targets and applications," *Nat. Rev. Microbiol.*, vol. 11, no. 6, pp. 371–384, 2013.

[128] S. Pal, Y. K. Tak, and J. M. Song, "Does the antibacterial activity of silver

nanoparticles depend on the shape of the nanoparticle? A study of the gram-negative bacterium Escherichia coli," *J. Biol. Chem.*, vol. 290, no. 42, pp. 1712–1720, 2015.

[129] T. C. Dakal, A. Kumar, R. S. Majumdar, and V. Yadav, "Mechanistic basis of antimicrobial actions of silver nanoparticles," *Front. Microbiol.*, 2016.

[130] V. E. dos Santos Junior *et al.*, "Antimicrobial activity of silver nanoparticle colloids of different sizes and shapes against Streptococcus mutans," *Res. Chem. Intermed.*, vol. 43, no. 10, pp. 5889–5899, 2017.

[131] S. Soares, G. Camino, and S. Levchik, "Comparative study of the thermal decomposition of pure cellulose and pulp paper," *Polym. Degrad. Stab.*, vol. 49, no. 2, pp. 275–283, 1995.

[132] Z. Xia, A. Singh, W. Kiratitanavit, R. Mosurkal, J. Kumar, and R. Nagarajan, "Unraveling the mechanism of thermal and thermo-oxidative degradation of tannic acid," *Thermochim. Acta*, vol. 605, pp. 77–85, 2015.

[133] A. Salam, L. A. Lucia, and H. Jameel, "Synthesis, characterization, and evaluation of chitosan-complexed starch nanoparticles on the physical properties of recycled paper furnish," *ACS Appl. Mater. Interfaces*, vol. 5, no. 21, pp. 11029–11037, 2013.

[134] C. Li, P. Sun, and C. Yang, "Emulsion stabilized by starch nanocrystals," *Starch/Staerke*, vol. 64, no. 6, pp. 497–502, 2012.

Appendix

A1 Alternative Additives and Softwood Pulp Tensile Tests

Tensile tests performed on hardwood pulp samples with additives (not shown in the main thesis) are shown in Figure A1-1. These additives were not included because they did not fit within the objectives or they contained incomplete or unverified data which would require more tests.

Furthermore, tensile tests performed on softwood pulp samples did not fit within the main theme of the thesis, due to a lack of data and unverified results. Additionally, these results contain some of the alternative additives that were described above. These results are shown in Figure A1-2.

The following codes apply for these figures:

- SWP – Softwood Pulp
- SCF - Short Cellulose Fibers
- Gx - Glyoxal
- A - Cationic StNPs
- B - Composite nanoparticles made by coextrusion of StNP “A” and Long Cellulose Fibers
- C - Aldehyde Functionalized StNPs
- D - Hydrophobic Functionalized StNPs
- E - SCF with grafted with polymerized acrylamide and 3-Acrylamidopropyl)trimethylammonium chloride
- F - Melamine Formaldehyde coated SCF

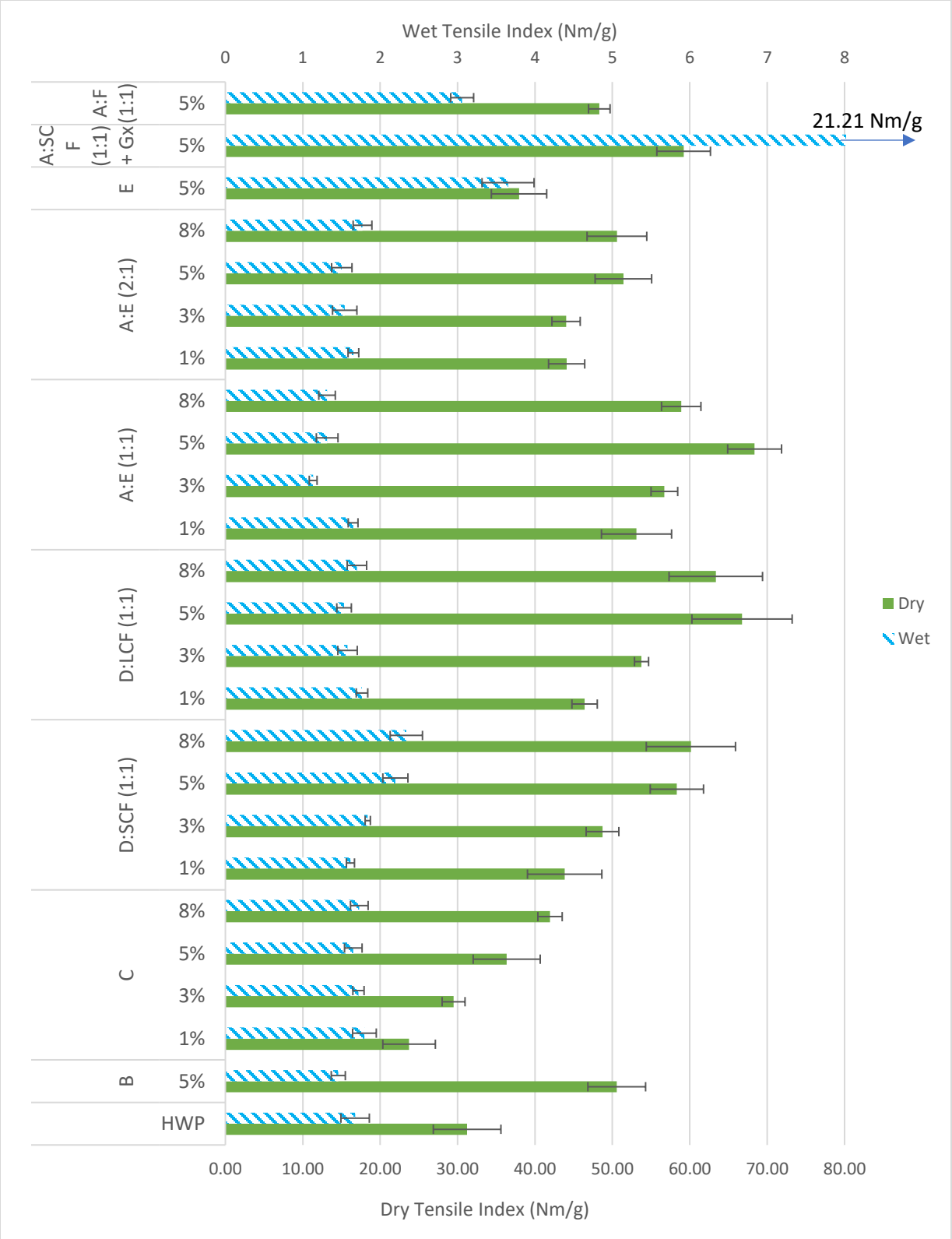

Figure A1- 1: Tensile index of hardwood pulp samples containing alternative additives.

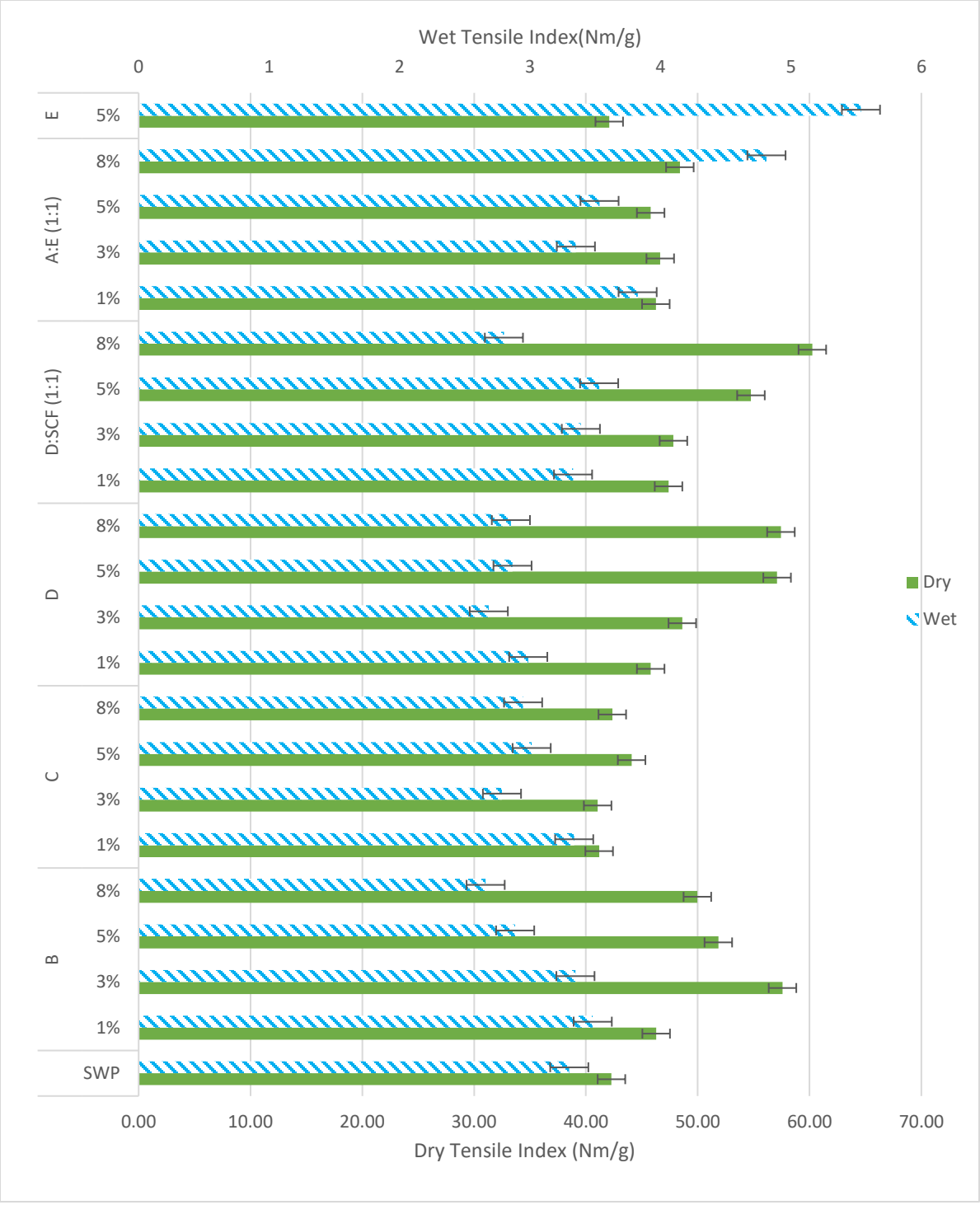

Figure A1- 2: Tensile tests of softwood pulp samples

From these results the following conclusions could be made:

- Softwood pulp is inherently stronger than hardwood pulp and the relative impact of the additives was reduced since the percent increases were smaller.
- The coextruded starch showed very good dry strength but minimal impact in wet strength, and the behaved like the original cationic StNPs
- Aldehyde modified StNPs had mixed results with an improved dry strength but minimal wet strength impact in the hardwood, and no visible trend was evident for the softwood samples
- While hydrophobically modified starch is shown in the main body of the thesis, using it in combination with short and long fibers was not shown.
    - In the softwood samples D:SCF (1:1) showed an increase in dry and wet strength, but the 8% sample showed an unexplained reduction in wet strength.
    - The hardwood samples showed D:SCF (1:1) as well, and demonstrated similar results as the A:SCF (1:1) shown in Chapter 3. However, the D:LCF (1:1) samples showed little to no improvement in the wet strength without a consistent trend. Both samples also displayed large standard deviations (> 6 Nm/g) in dry strength bringing the reliability of the results in question.
- SCF with grafted poly-acrylamide and (3-Acrylamidopropyl)trimethylammonium chloride was prepared by Dr. Yao while working on this project. The materials, procedure, and quantities were not provided for this material. By itself, it showed

very high wet strength improvements but when mixed with cationic StNPs almost all the wet strength improvement disappeared.

- Hand sheets dipped in a solution of glyoxal gained wet strength that far surpassed any other wet strength. This wet strength was shown to be temporary in Figure A1-3 by taking samples with StNP 'B' dipped in glyoxal and soaking them in water for various lengths of time. The safety of using this product is questionable and thus, it does not fit into the theme of the thesis.
- Finally, melamine formaldehyde coated SCF was produced by Dr. Mohammed where, again, the methods to produce this material were not provided. This system was capable of providing improvements in wet strength when used with cationic StNPs, but only one sample was prepared and tested.

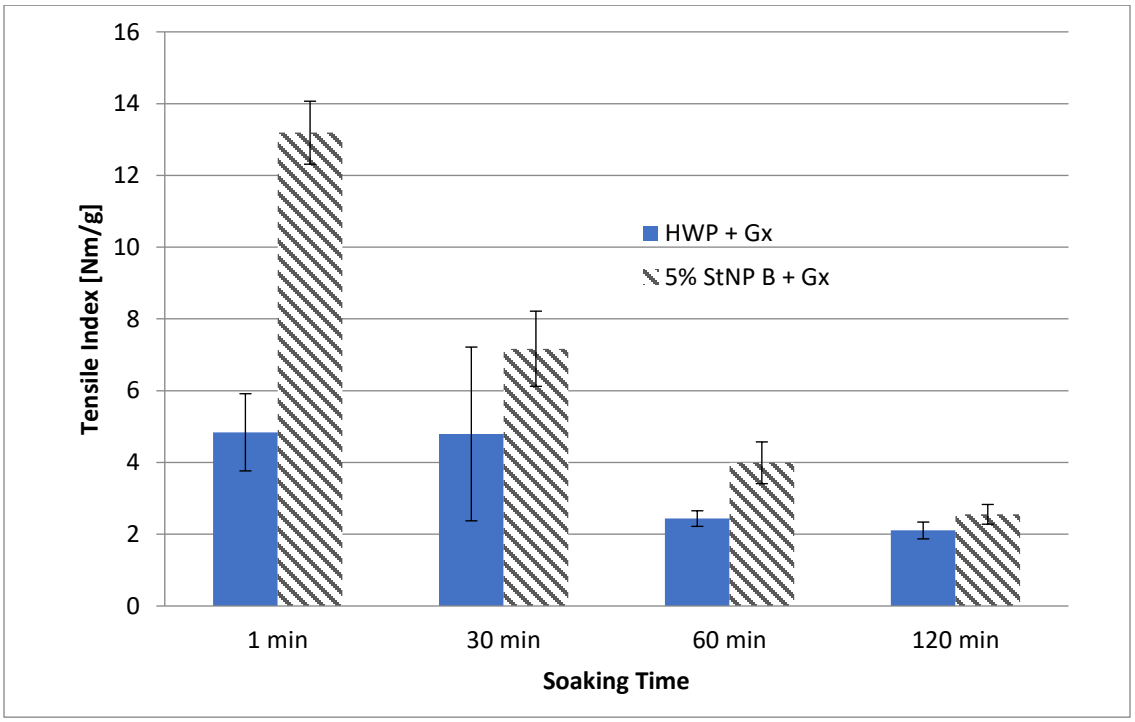

Figure A1- 3: Tensile results of soaked glyoxal dipped hand sheets at various soaking times.

A2 Methyl Orange Test

To determine if the hydrophobic starch had detached from the pulp matrix when exposed to water, a test was devised. The starch was dyed with methyl orange (MO) and tested by UV-Vis to determine the amounts of starch loss from the pulp. The following procedure was developed:

First 0.1 wt.% StNPs were dispersed in DI water, and 100 mg/L MO was added to the mixture. The dispersion was dialyzed for one week with water changed twice daily. After dialysis, the normal hand sheet preparation process was used. A small amount of the dialyzed sample was kept as a reference to prepare a calibration curve for UV-Vis measurements at a wavelength of 461 nm. The absorbance was converted to concentration using this calibration curve.

Two samples with 5 and 10 wt.% StNP were prepared for this test. After the normal hand sheet formation process, an aliquot of the filtrate was collected, and the total volume measured. The hand sheets were dried placed in a Buchner funnel and 50 mL of DI water was passed through the sample to measure the concentration of MO.

The results of this test are shown in Figure A2-1 and Table A2-1. The results suggested that the amount of StNPs loss during the filtration step was higher than the amount of starch added, and that there was a detectable amount of StNP when passing water through the paper in the Buchner funnel. The reasons these results might have occurred could be the followings:

1. The MO may become detached from the StNP when dispersed in the pulp slurry. Thus, the absorbance in the filtrate would not correlate with the calibration mixture.
2. The starch/MO mixture may not have the same electrostatic attraction to the pulp, and this may result in the greater loss of starch than normal.

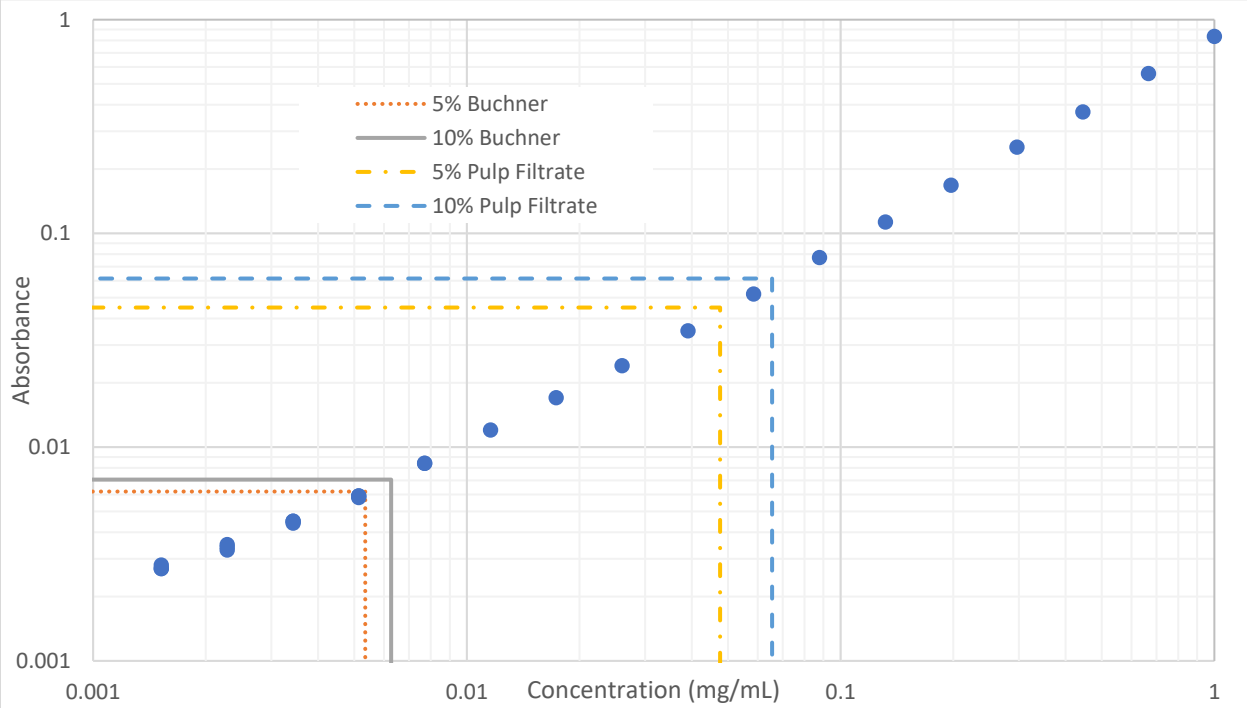

Figure A2- 1: UV-Vis results showing the concentration of hydrophobic starch plotted against a calibration curve.

Table A2- 1: Calculations based on the Methyl Orange Test

Sample Name	Volume (mL)	Concentration (mg/mL) [x10^{-3}]	Starch Lost (mg)	Starch Added
5% Buchner	50	5.35	0.27	
10% Buchner	50	6.27	0.31	
5% Pulp Filtrate	1175.5	47.6	55.95	37.5
10% Pulp Filtrate	1178.8	65.6	77.29	75

A3 Dynamic and Static Light Scattering of Hydrophobic Starch

To examine the aggregation behaviour of the hydrophobic StNPs, dynamic light scattering (DLS) and static light scattering (SLS) was performed. The results were unreliable due to the data requiring a quadratic fit to the SLS results. Additionally, because of the turbidity of the solution, very low concentrations of StNPs were used, and the results were not representative to the behaviour during the paper making process. Regardless, the DLS results demonstrated a hydrodynamic radius (R_h) of about 71 nm and the SLS results showed a radius of gyration of 229 nm. The data for these results are shown in Figure A3-1 and Figure A3-2. Where R_h can be calculated using the following equation:

$$R_h = \frac{k_B T q^2}{6\pi\eta\Gamma}$$

where k_B is the Boltzmann constant, T is the temperature in Kelvin, η is the fluid viscosity of water, Γ is the decay rate and q is the wave vector. The slope of $\frac{\delta\Gamma}{\delta q^2} = 2.02448 \times 10^{-12}$ which is equaled to the diffusion coefficient D_T.

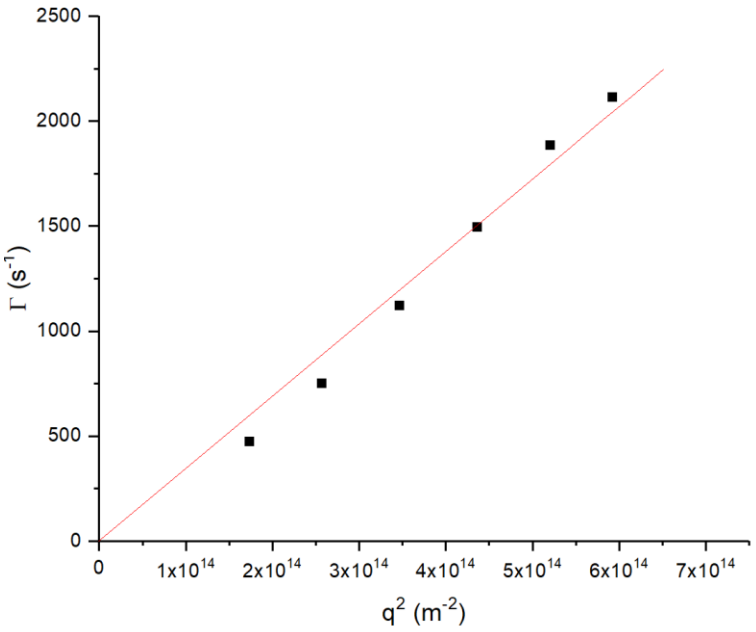

Figure A3- 1: Dynamic light scattering results for the hydrophobic StNPs.

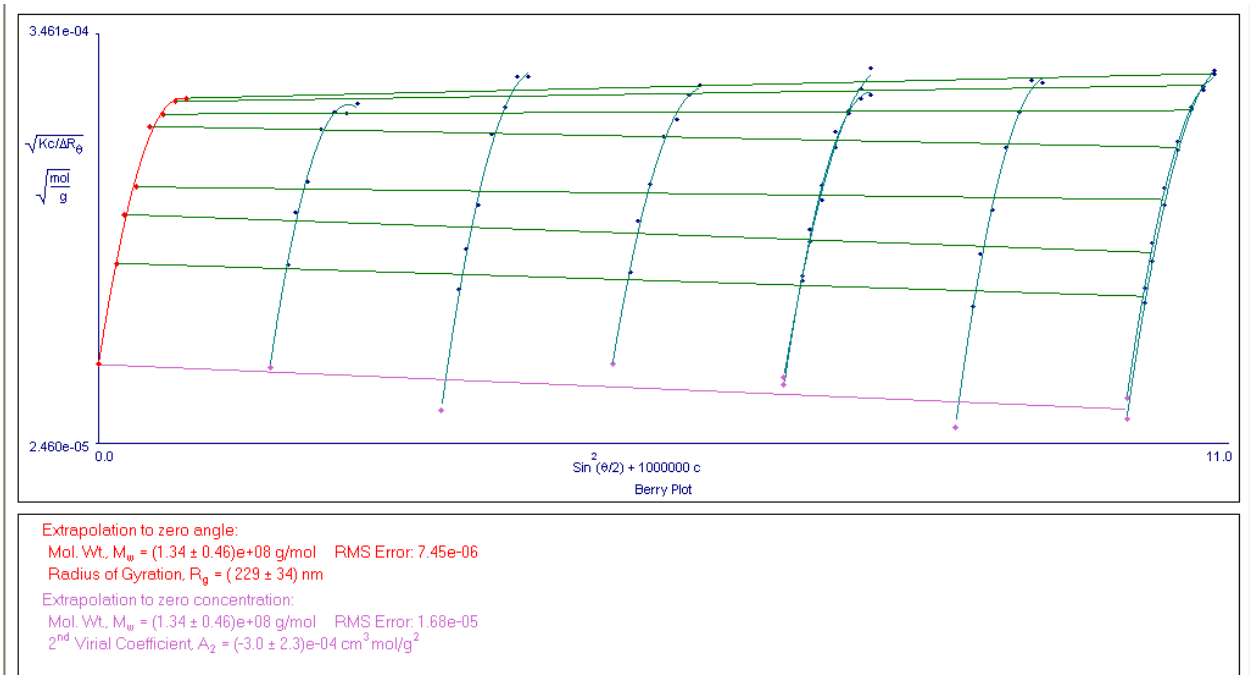

Figure A3- 2: Static light scattering results for the hydrophobic StNPs.

A4 Zeta Potential Differences

Since the pulp and the additives possessed opposing zeta potentials, it would be interesting to study the zeta potentials before and after filtration. In Figure A4-1 the zeta potential of the base components for the hand sheets were measured. Only the cationic starch nanoparticles (StNPs) were positive, while the hardwood pulp (HWp), softwood pulp (SWp), long and short cellulose fibers (LCF, SCF) were negative.

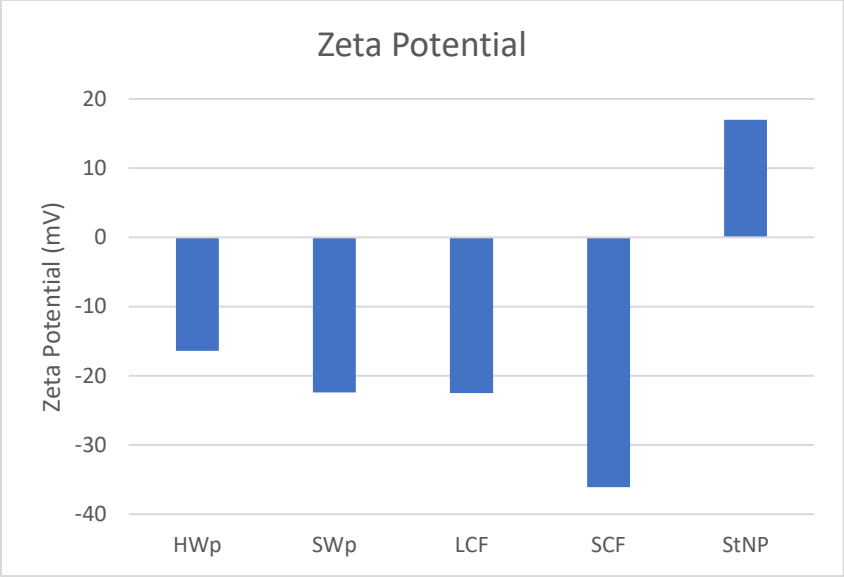

Figure A4- 1: Zeta potential measurements of base components in the hand sheet

The difference in zeta potential could provide information on the behaviour of the StNPs before and after filtration. The difference was calculated by the formula below:

$$\zeta_{difference}(mV) = \zeta_{filtrate} - \zeta_{sample}$$

In this way, if the difference is negative, it implied that there is a higher ratio of positive components in the sample feed than in the filtrate. This occurs under a combination of the following conditions:

a) The positive components were strongly bound to the pulp hand sheet, and thus, were present into the filtrate
b) The negative components were not retained in the filter mesh and passed into the filtrate.

Therefore, it would be ideal for the difference to be negative as this means the StNPs were mostly retained in the pulp hand sheet. Figure A4-2 shows the zeta potential difference of several samples where the zeta potential was measured. For StNPs alone, the zeta potential was positive, implying a loss of StNPs. However, when mixed with SCF or LCF in a 1:1 ratio, the zeta potential was negative. This indicated a higher retention of the positive StNPs when used in conjunction with these cellulose fibers. The results reported in Chapter 3 supported this observation, and the use of LCF or SCF improved the tensile strength, which is likely due to a higher retention of components.

These results were not included in the main body of the thesis since many of the tested formulations did not have corresponding zeta potential data. Additionally, some of these results were conducted by the postdoctoral researcher before I had started working on the project.

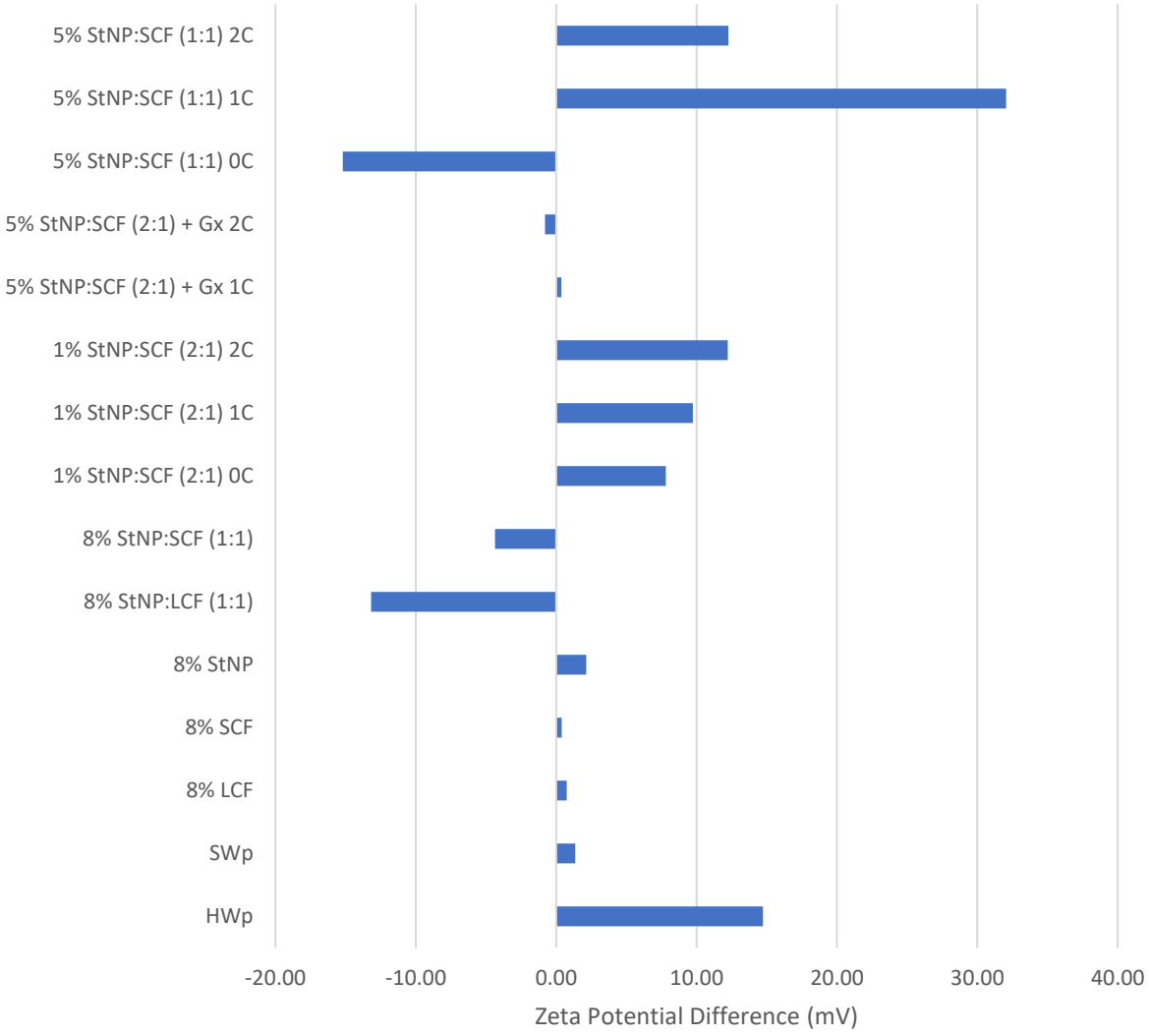

Figure A4- 2: Zeta potential difference of various tested samples

A5 Starch Nanoparticle Distribution

Figure A5-1 shows a TEM image taken by Dr. Yao before I had started working on this project. A large quantity of StNPs are shown to be evenly distributed across the SCF and pulp network. However, the concentrations and procedures used to prepare this image are unknown. Nevertheless, this result verifies that the StNPs can form an electrostatic coating on the fibers and consequently used as a binder to strengthen the inter-fiber bonds. Additionally, this finding supports the tensile results presented in Chapter 3 by revealing the mechanism involved in increasing the hand sheet tensile strength.

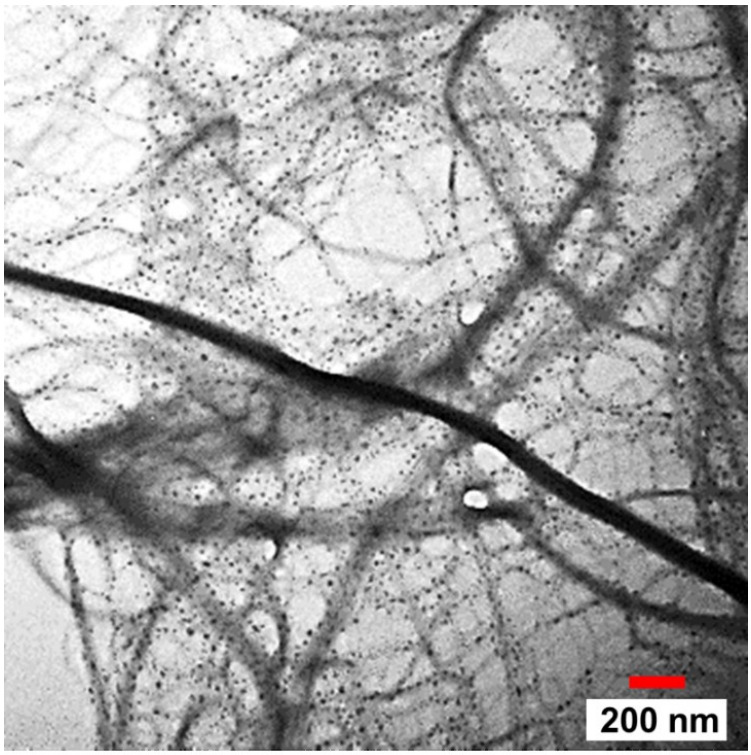

Figure A5- 1: TEM of stained cationic StNPs (black dots) in a SCF and HWp network